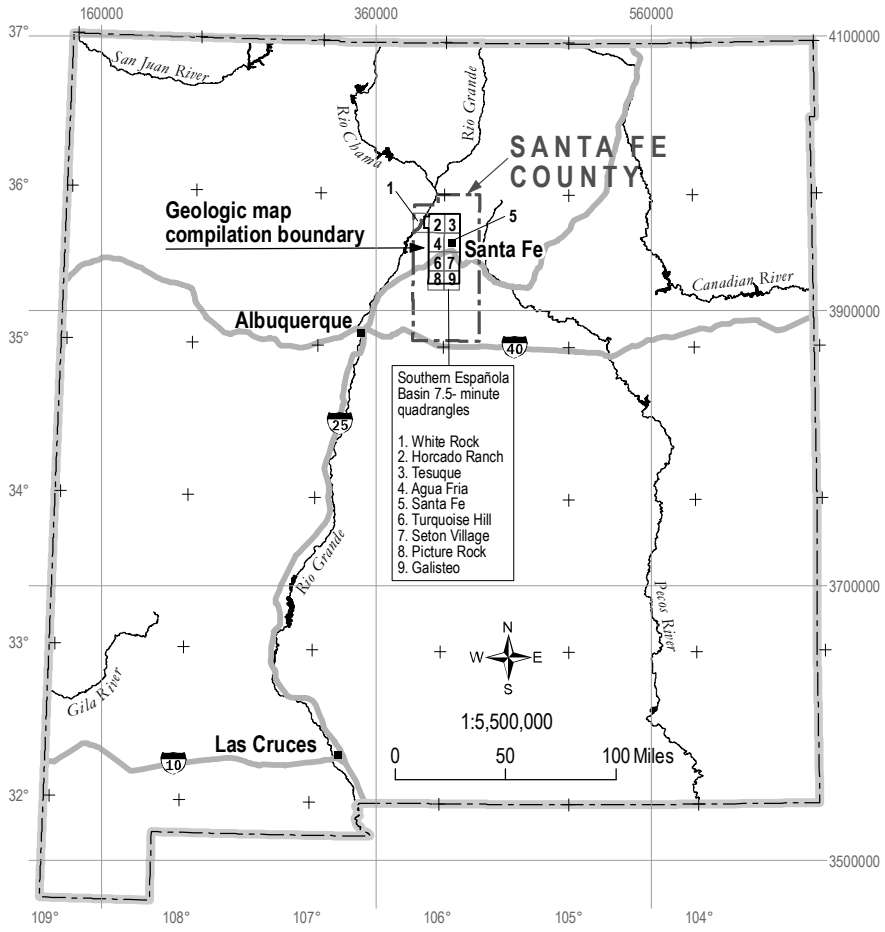

Figure 1–Index map for New Mexico and the study area in the southern Española Basin.

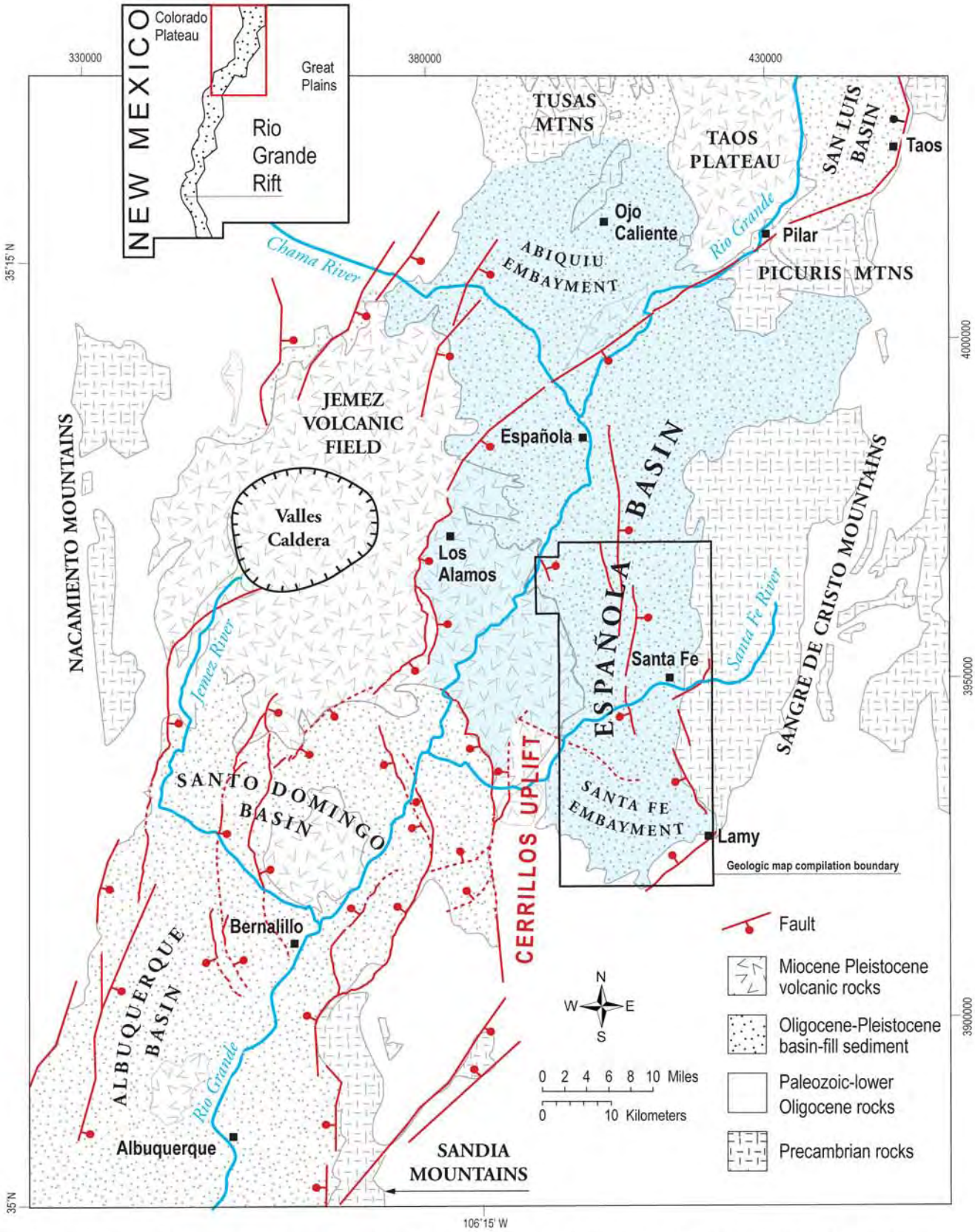

Figure 2–Regional geologic setting of the Española Basin (some geologic features from Read etal. 2004 and Sawyer and Minor 2006)

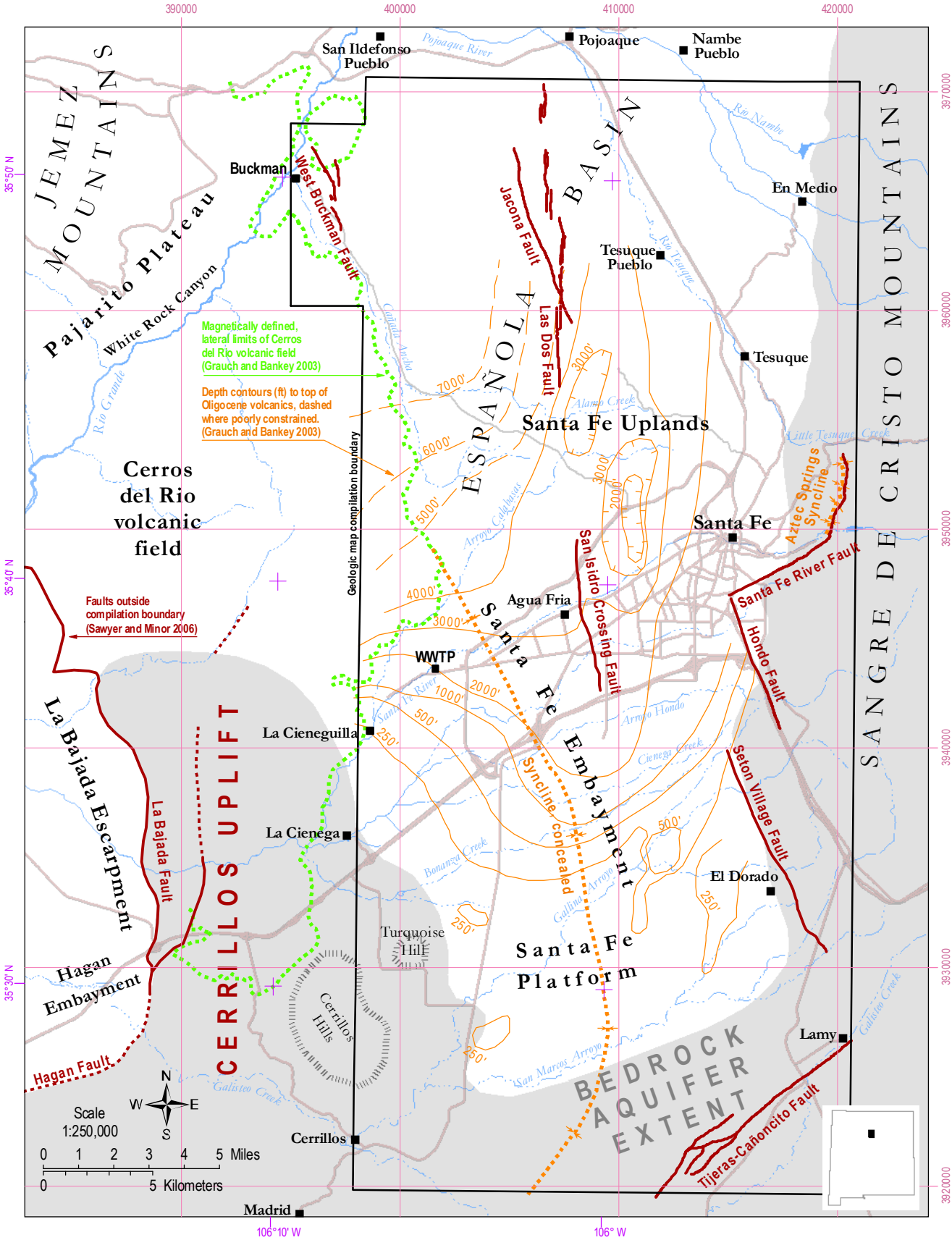

Figure 3–Select physiographic and tectonic features for the southern Española Basin.

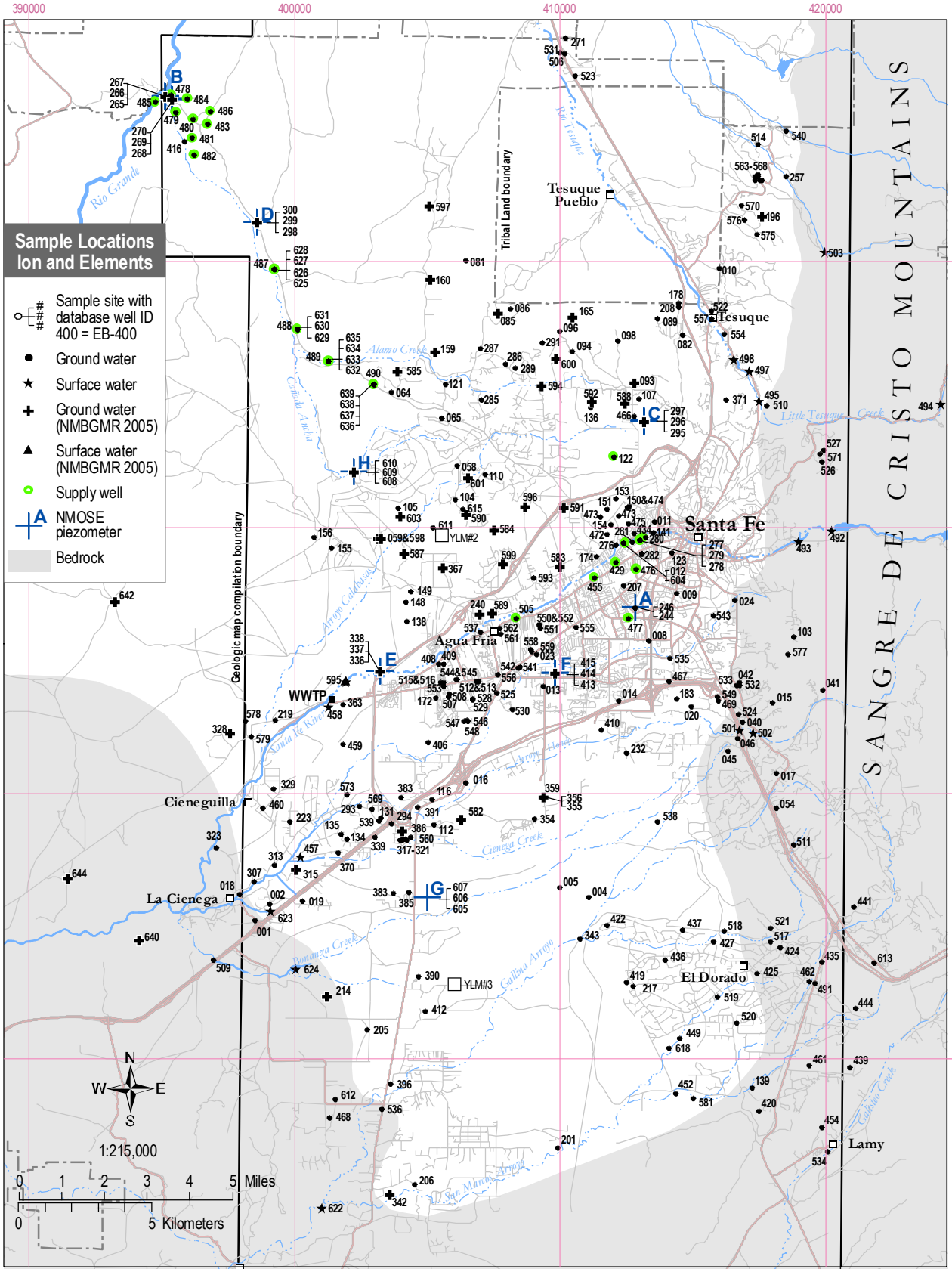

Figure 4– Locations of ground water and surface water samples collected and data compiled for ion and trace chemistry in the southern Española Basin.

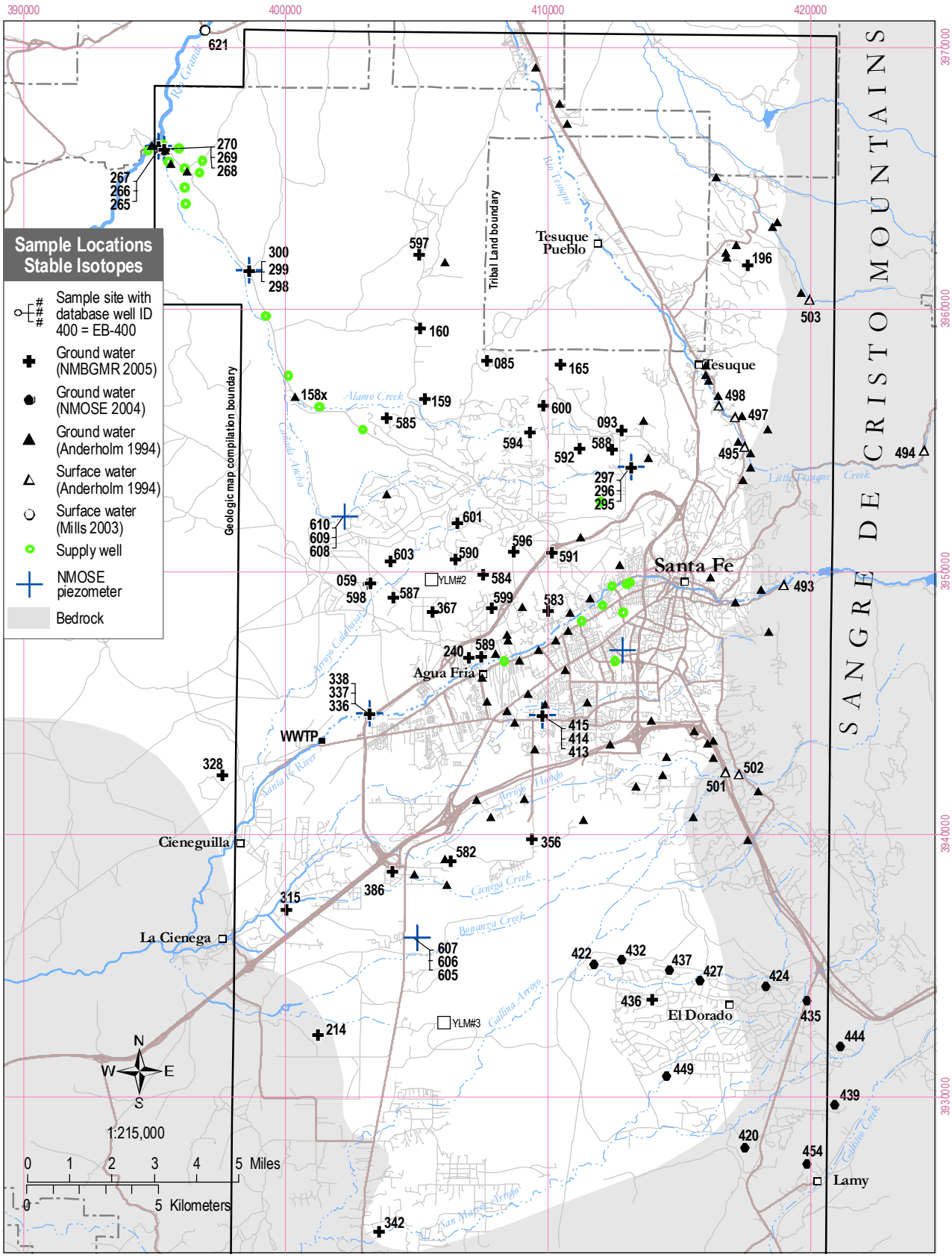

Figure 5– Locations of ground water and surface water samples collected and data compiled for stable isotope chemistry in the southern Española Basin.

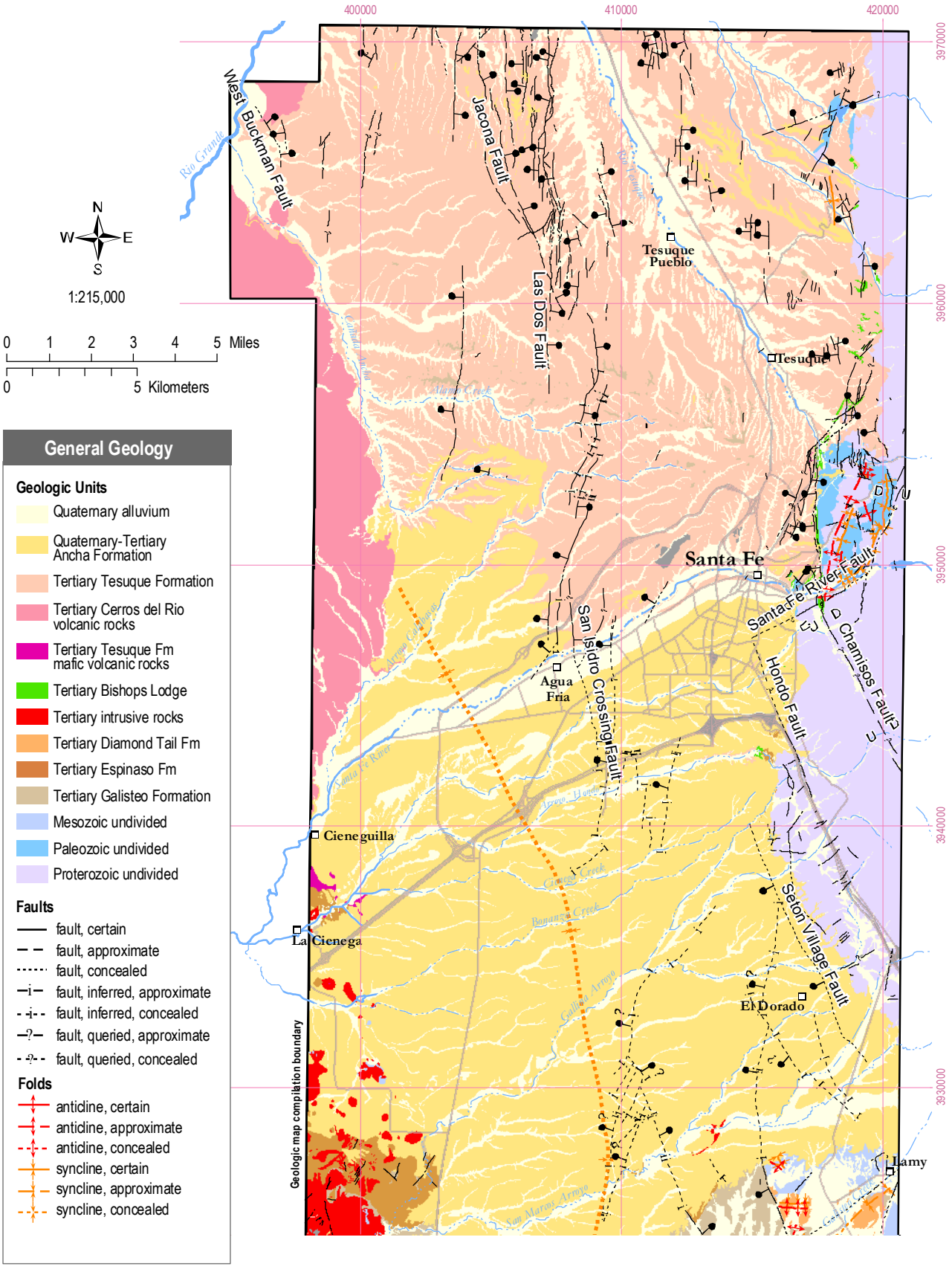

Figure 6–Generalized geologic map of the southern Española Basin (modified from Read et al. 2004).

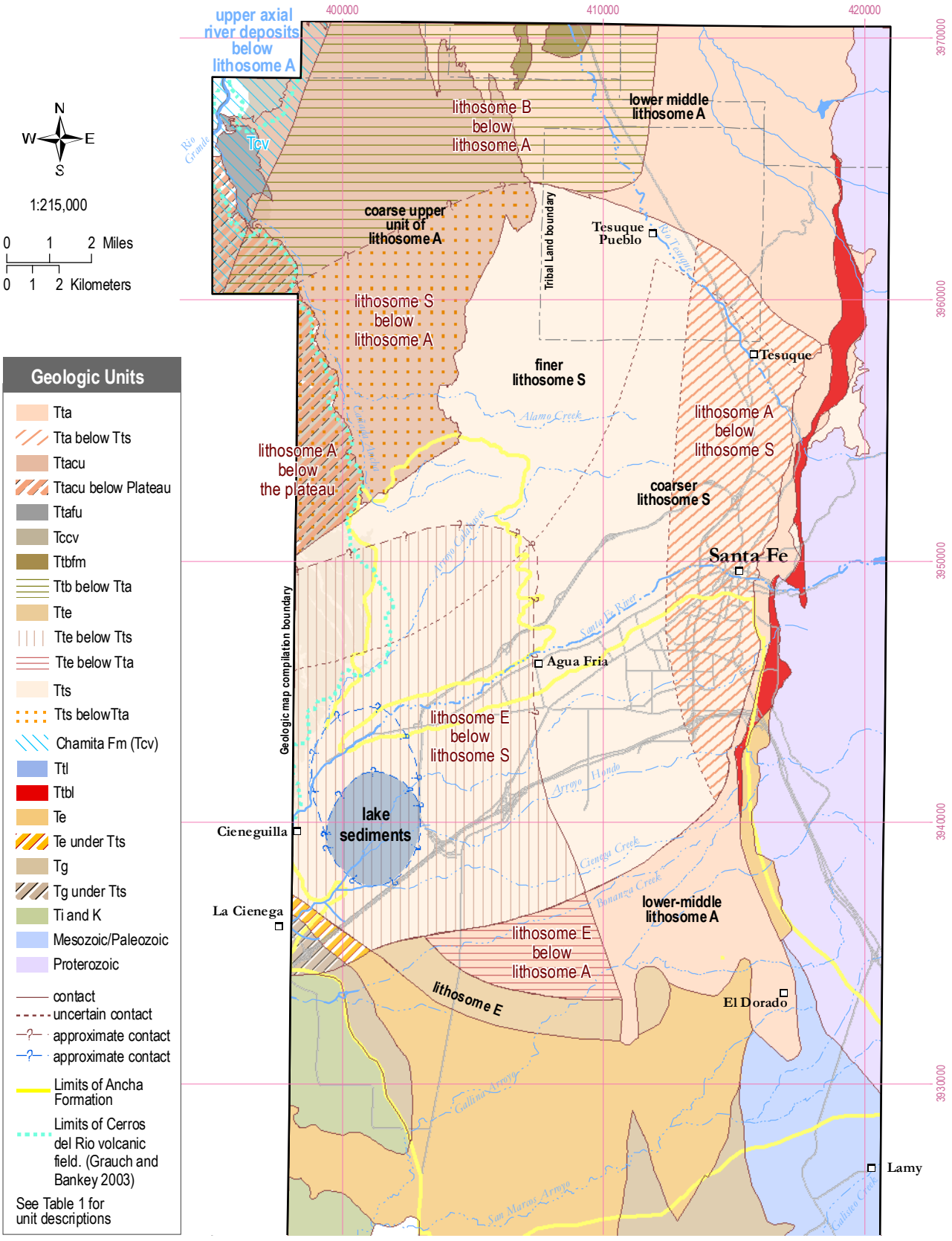

Figure 7– Generalized subcrop map (Quaternary units and Ancha Formation removed) showing the spatial distribution of lithosomes A, B, E, S, and lake sediments in the Tesuque Formation (from Koning and Johnson 2006).

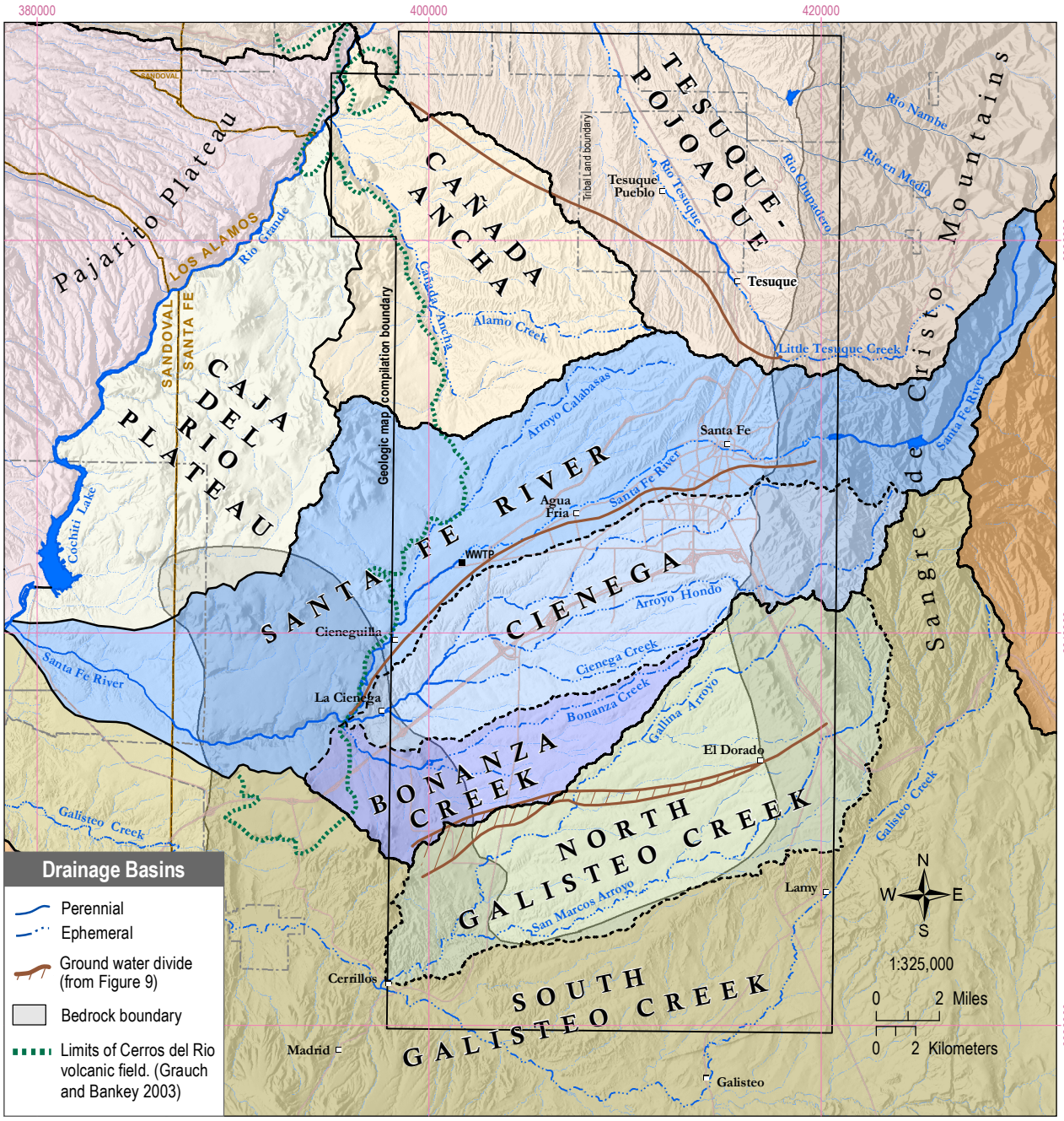

Figure 8–Drainage basins and perennial and ephemeral stream courses in the southern Española Basin.

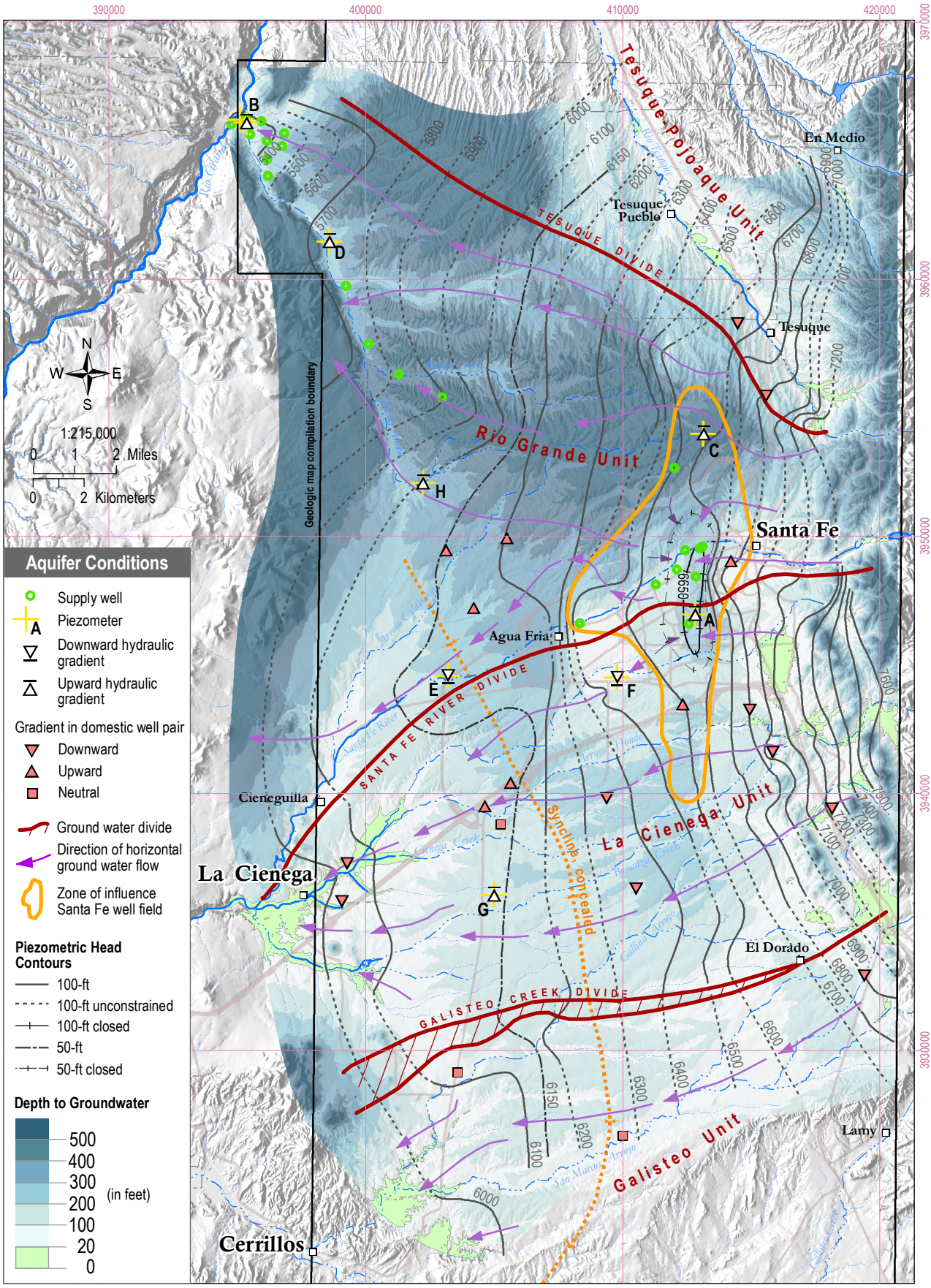

Figure 9–Ground water flow conditions in the Tesuque aquifer system, Santa Fe area.

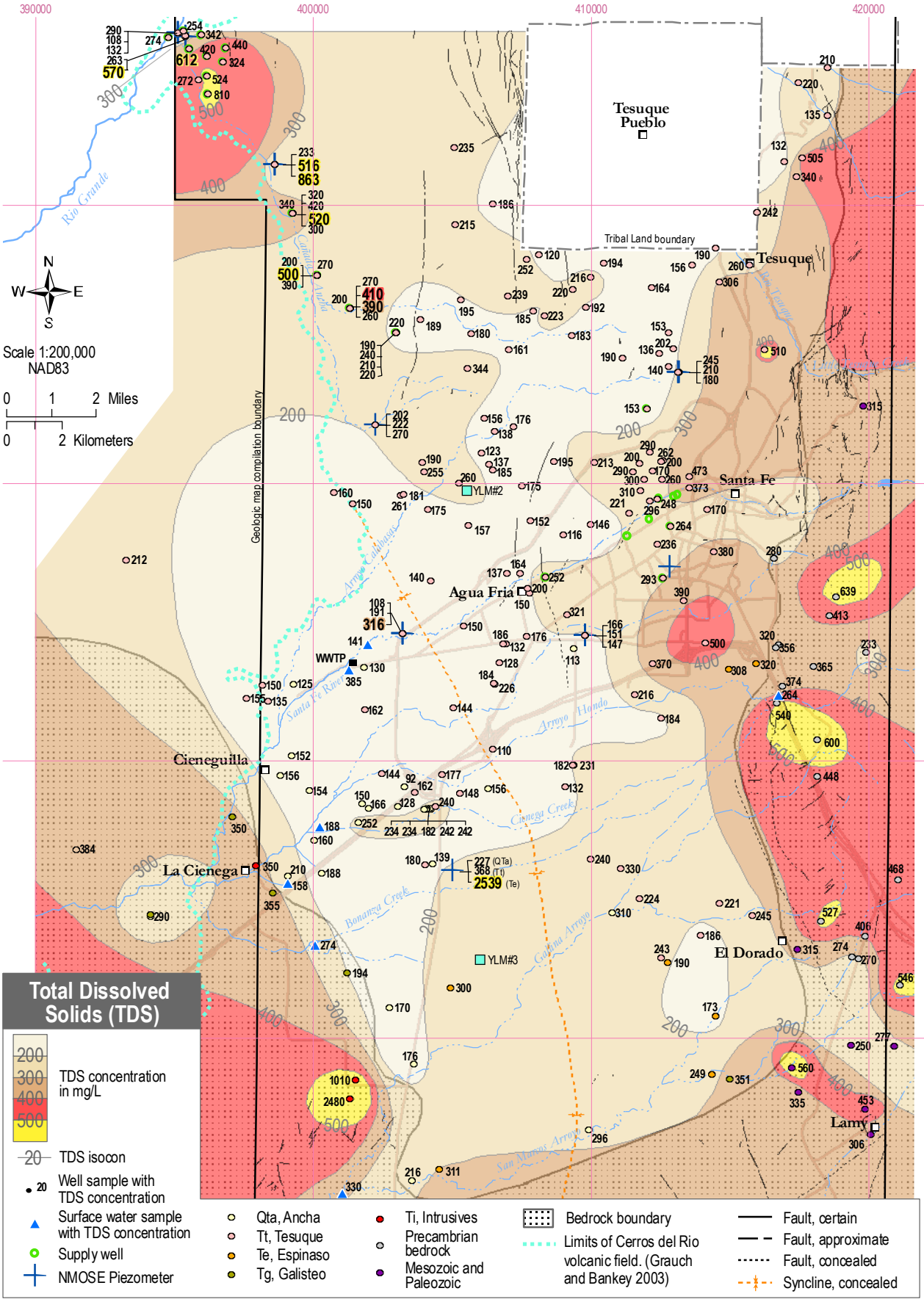

Figure 10–Concentration of total dissolved solids for ground water in the southern Española Basin.

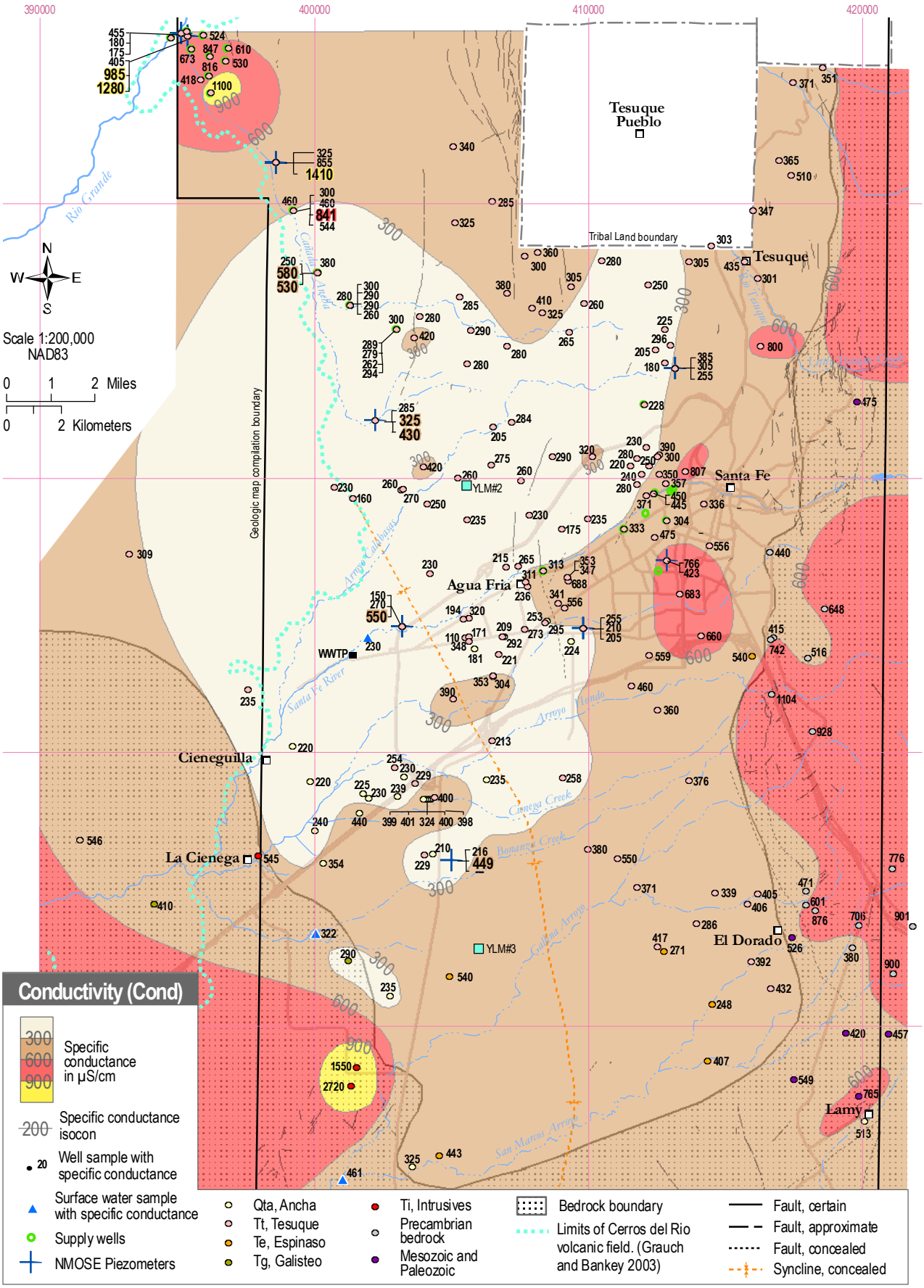

Figure 11–Specific conductance for ground water in the southern Española Basin.

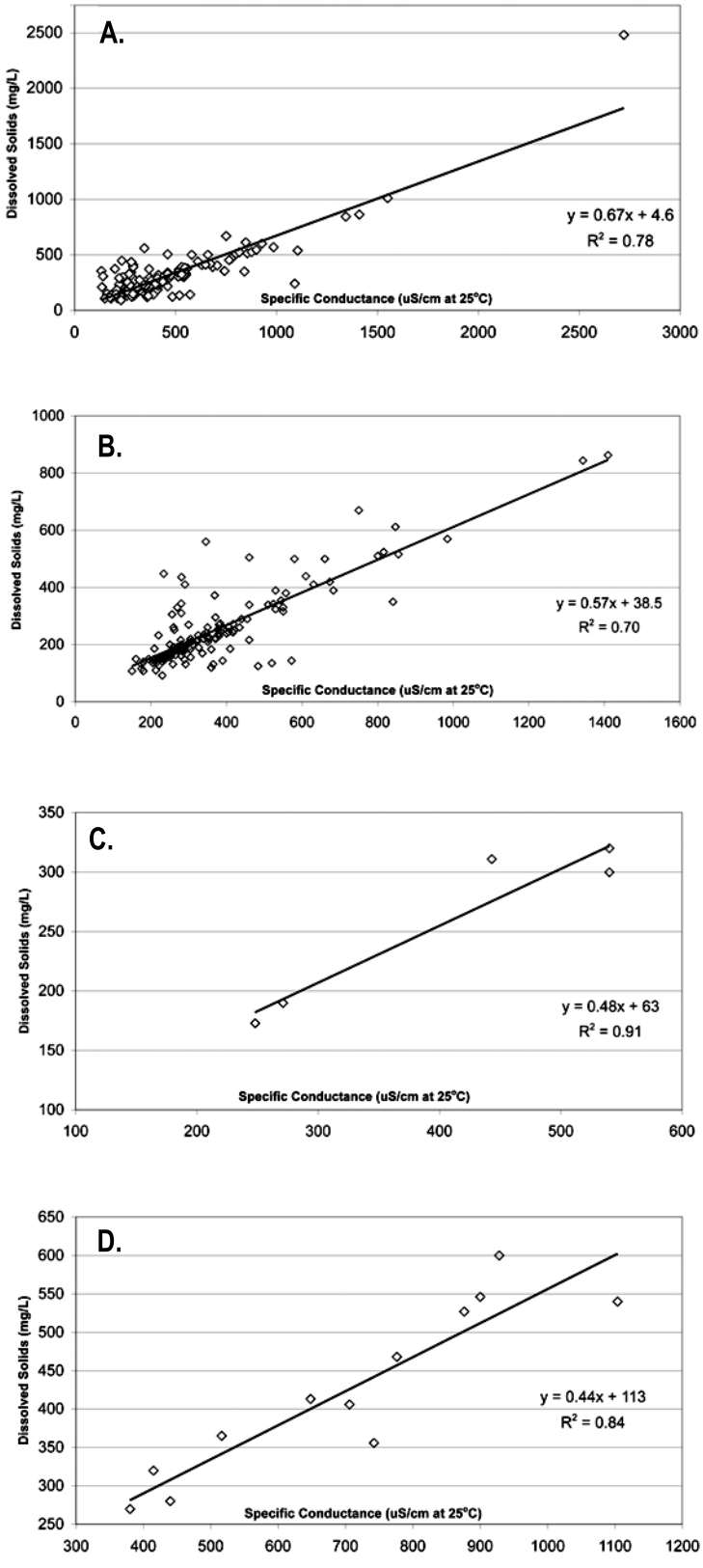

Figure 12--Plots of total dissolved solids versus specific conductance for: (A) all water samples; (B) Tesuque Formation ground water; (C) Espinaso Formation ground water; and (D) Embudo Formation ground water.

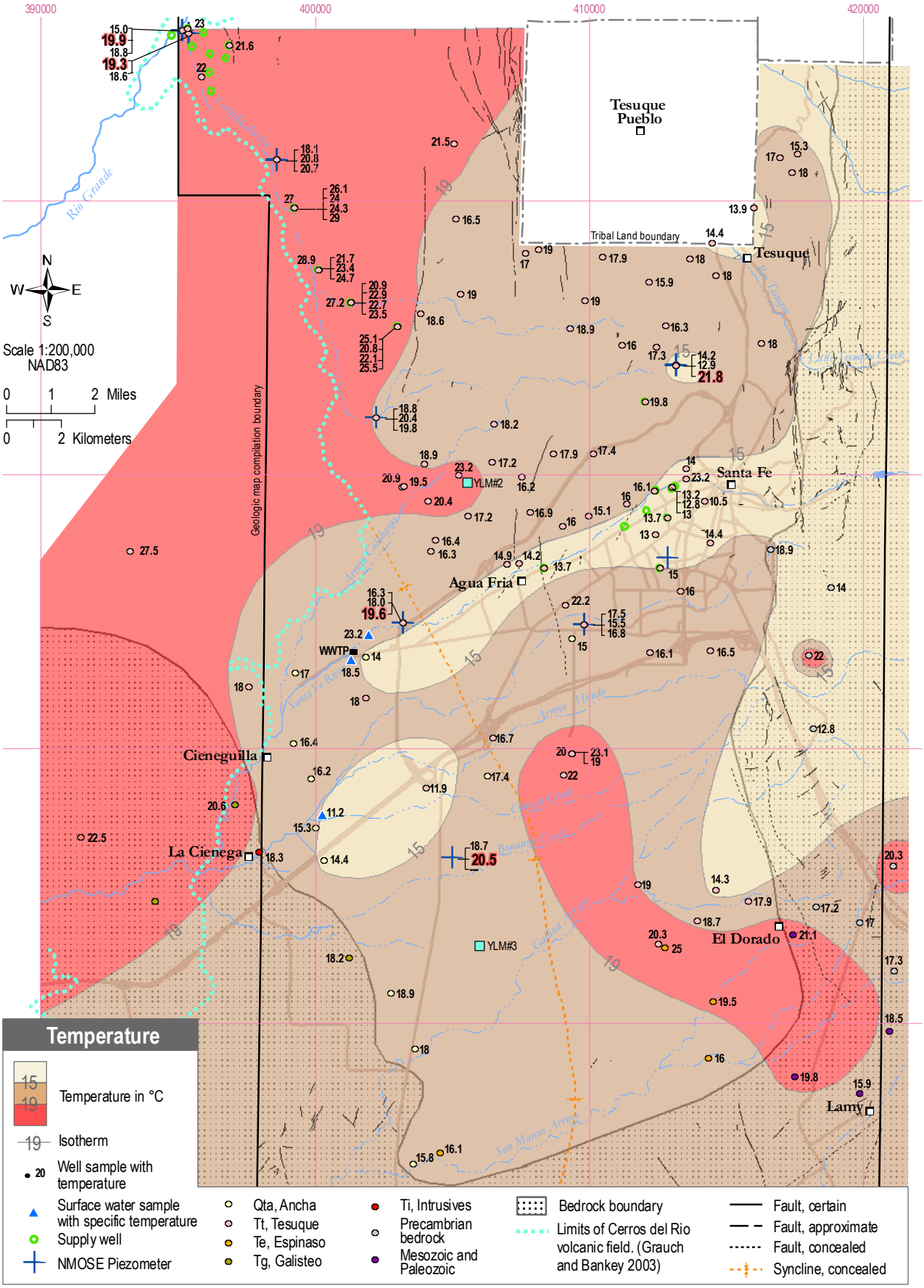

Figure 13–Temperature of ground water in the southern Española Basin.

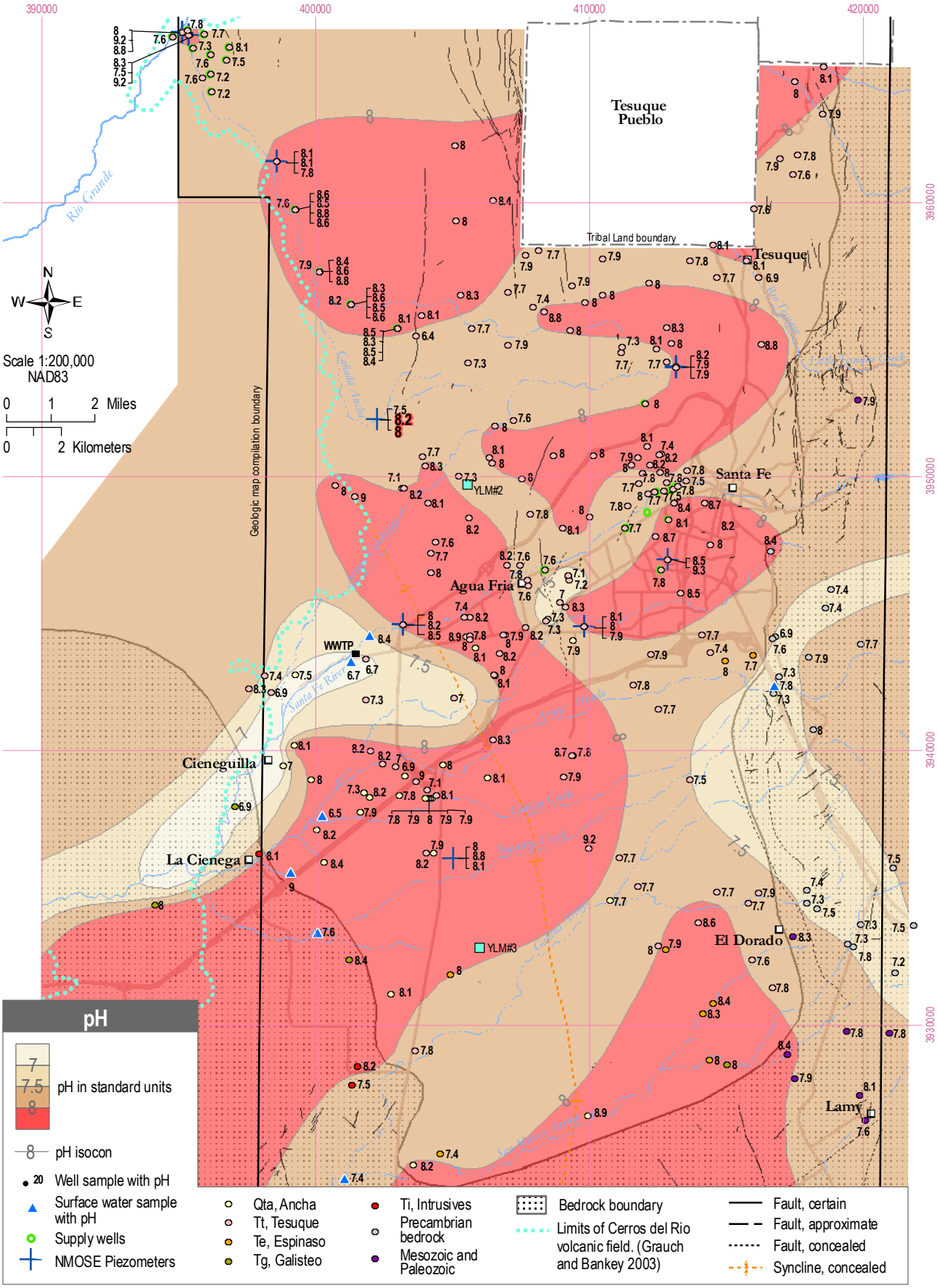

Figure 14–pH for ground water in the southern Española Basin.

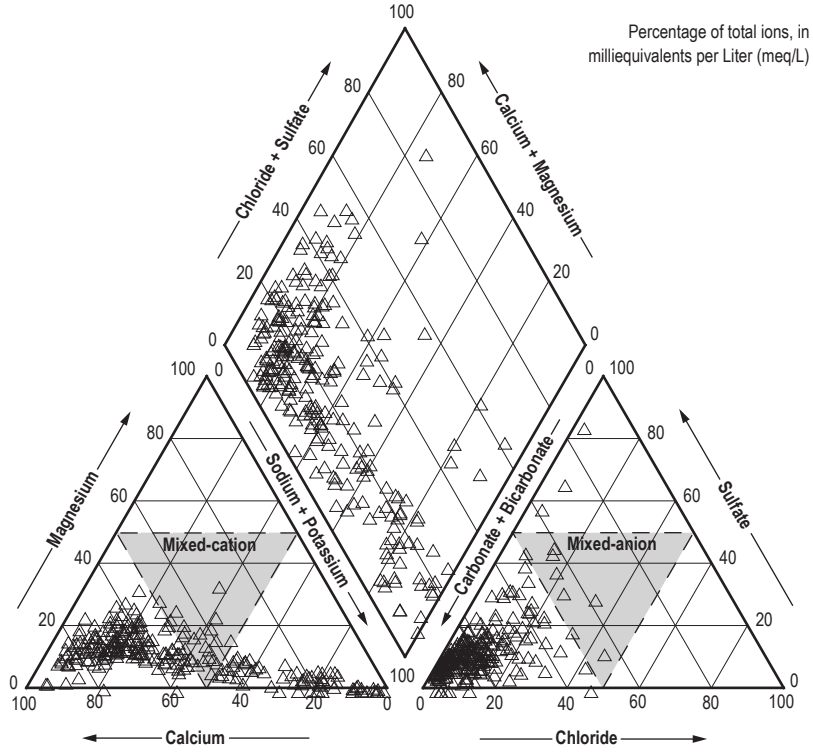

Figure 15–Piper diagram showing water types for all ground water and surface water samples from the Santa Fe area.

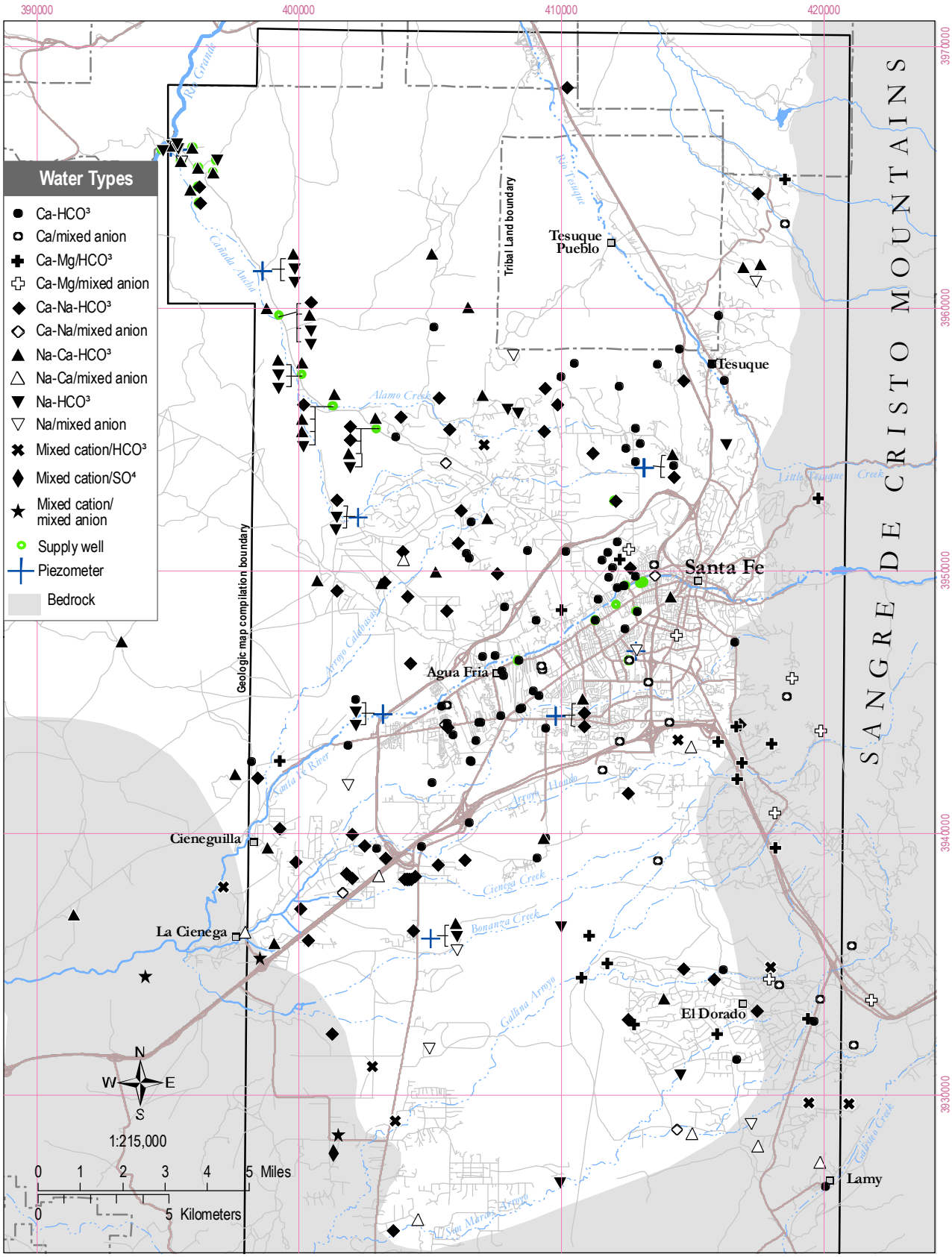

Figure 16– Water types of ground water and surface water samples in the Tesuque Formation and bedrock units in the southern Española Basin (based on the piper diagram of Figure 15).

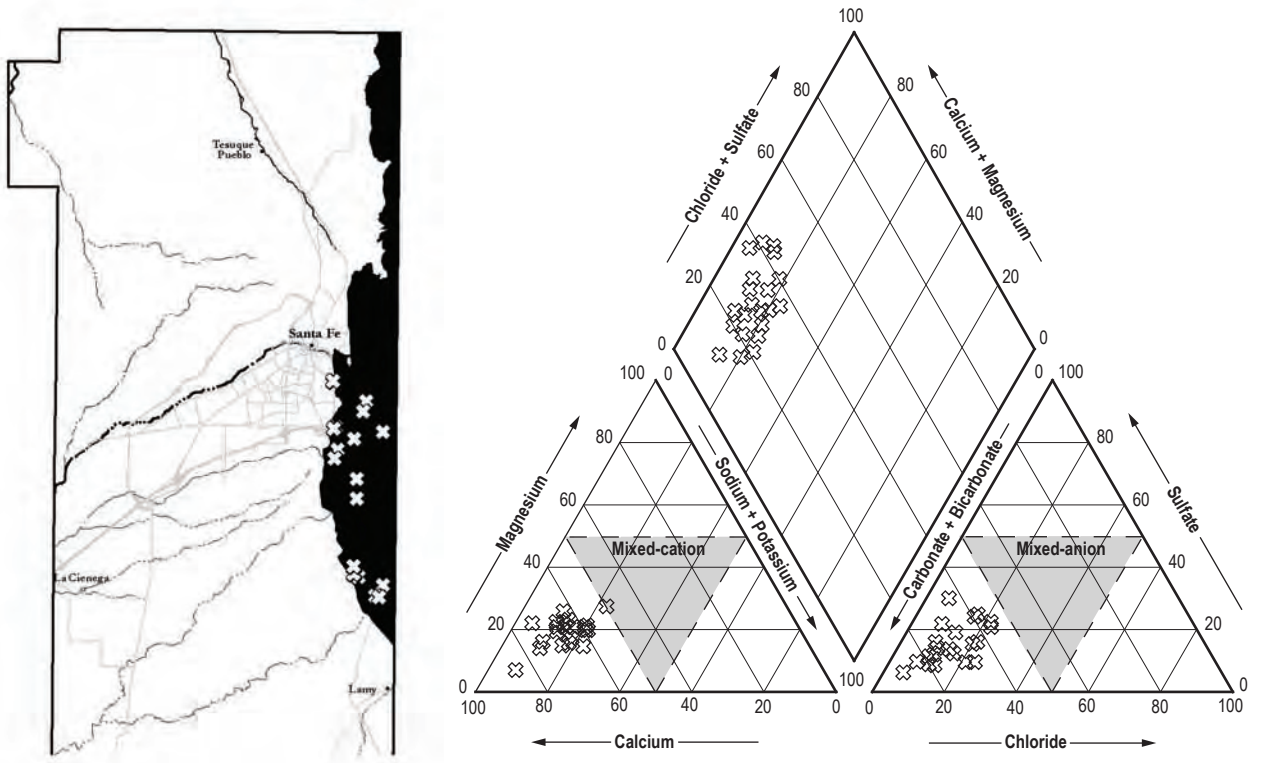

Figure 17– Piper diagram for ground water samples from Proterozoic granitic rocks of the Embudo formation. The dominant water type in the Embudo formation is calcium-magnesium-bicarbonate, with minor enrichment of sulfate and chloride.

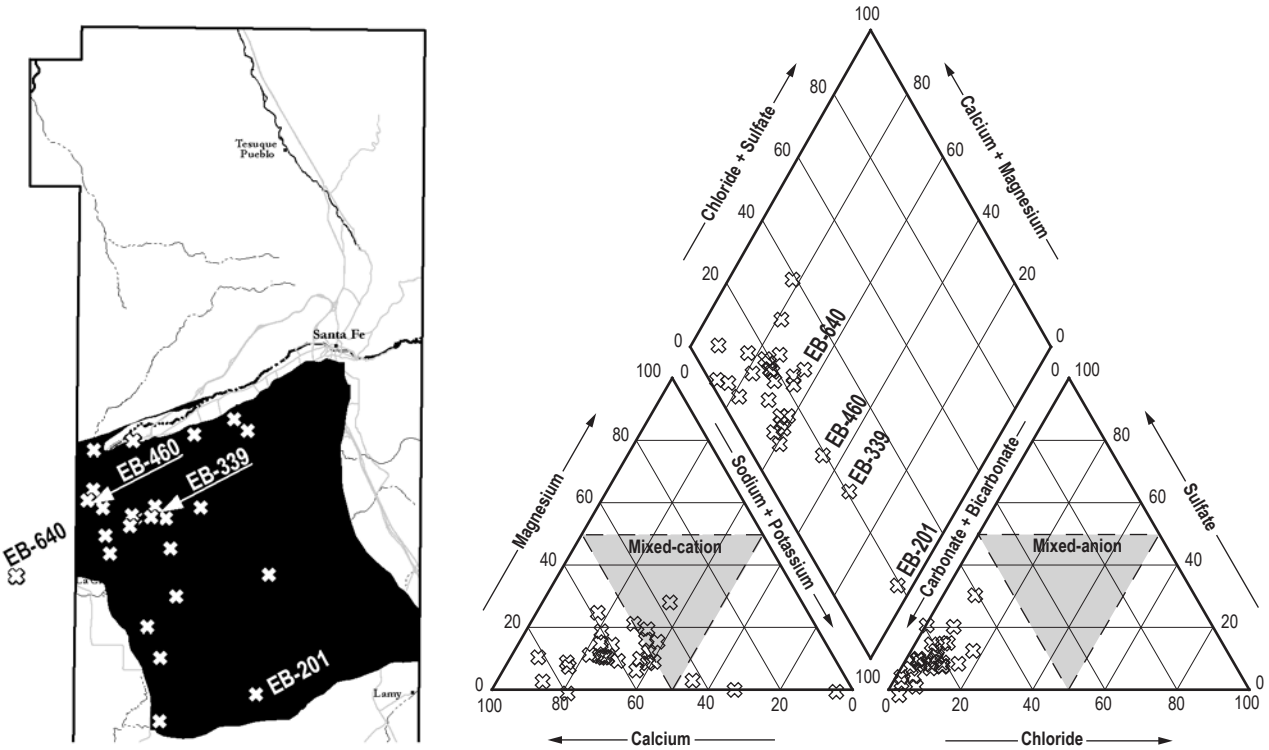

Figure 18–Piper diagram for ground water samples from the Ancha Formation. The dominant water type in the Ancha Formation aquifer is calcium-sodium-bicarbonate. Sodium enrichment is probably associated with mixing of ground water from adjacent formations, as in samples EB-201, EB-339, EB-460 and EB-640.

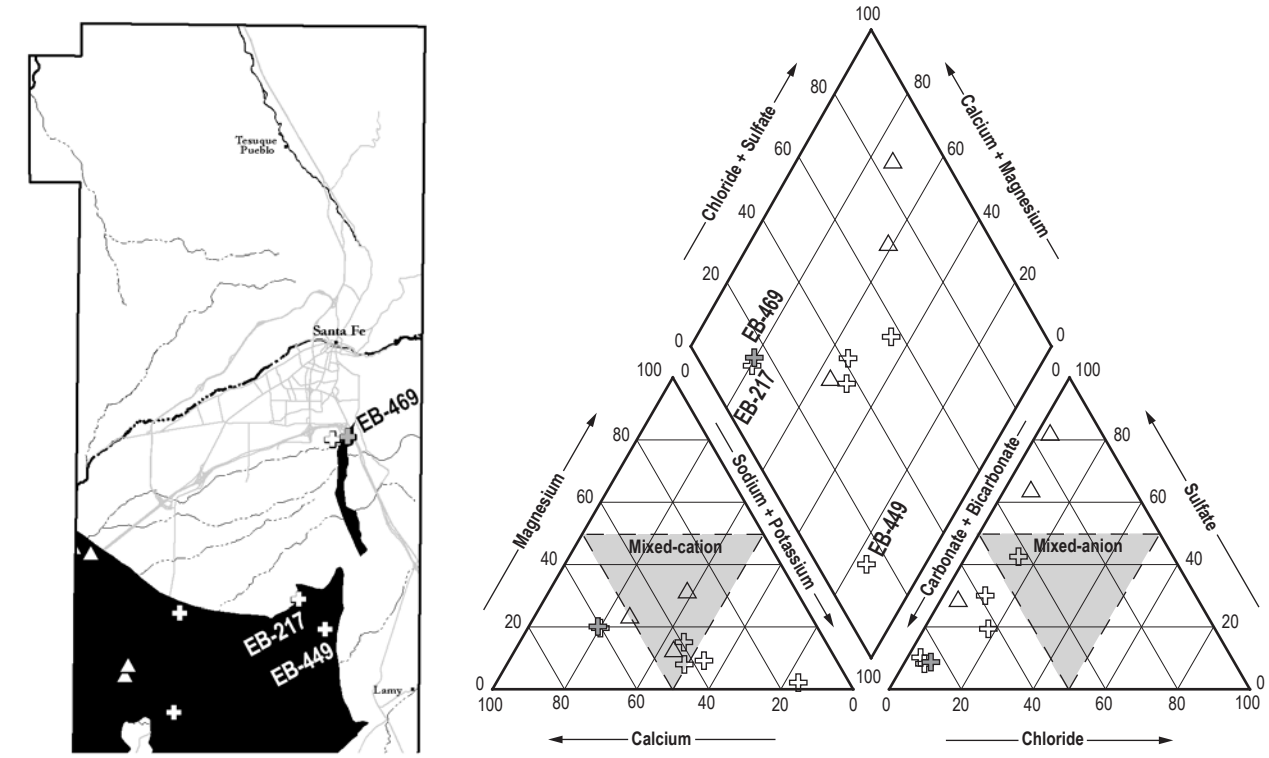

Figure 19–Piper diagram for ground water samples from the Espinaso Formation (✣), Espinaso/Embudo Formation (✣) and other Tertiary volcanic rocks (△). The dominant water types in these volcanic and volcaniclastic formations are calcium-sodium and sodium-calcium bicarbonate, with occasional enrichment of sulfate.

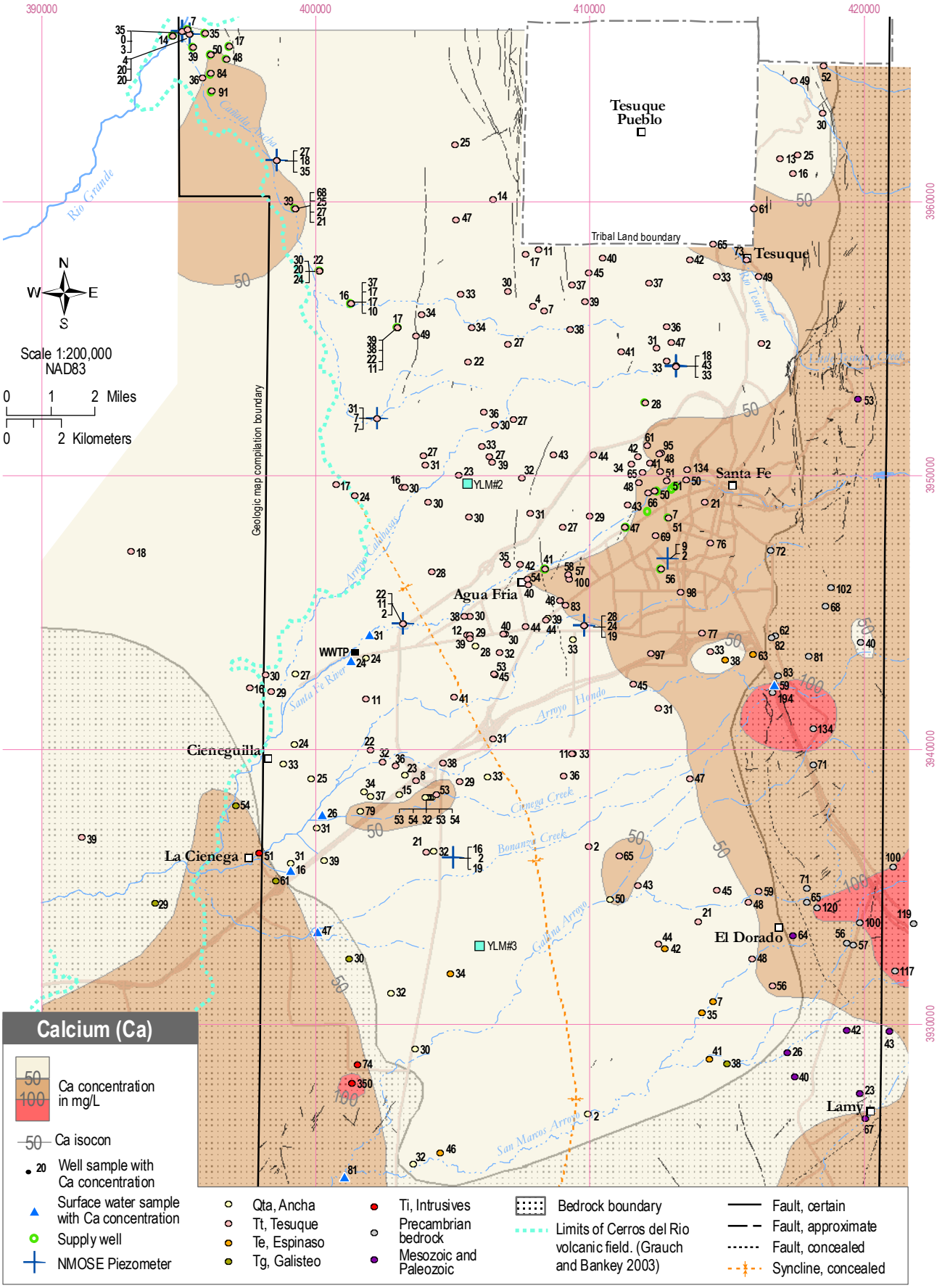

Figure 20–Calcium concentration for ground water in the southern Española Basin.

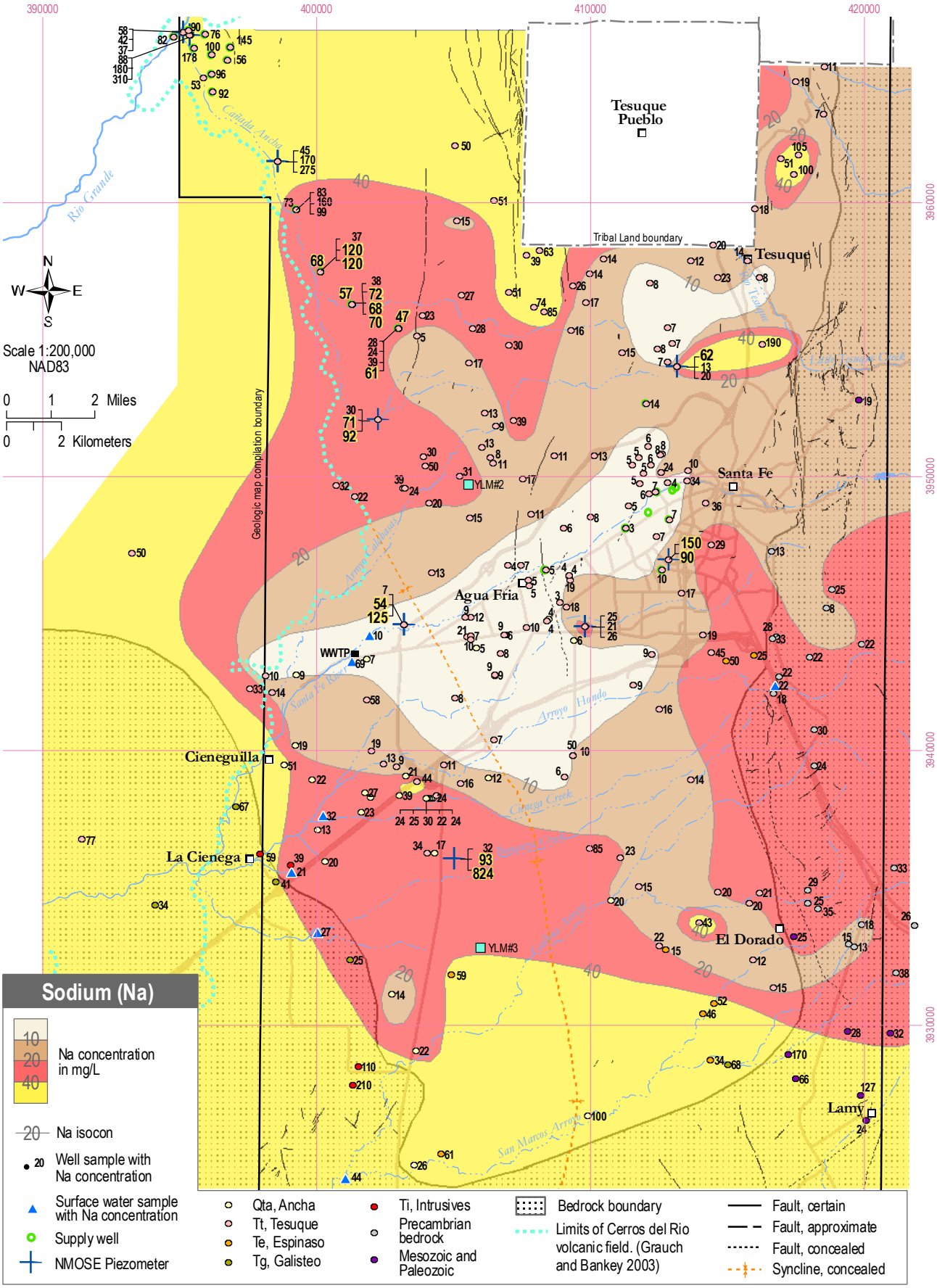

Figure 21– Sodium concentration for ground water in the southern Española Basin.

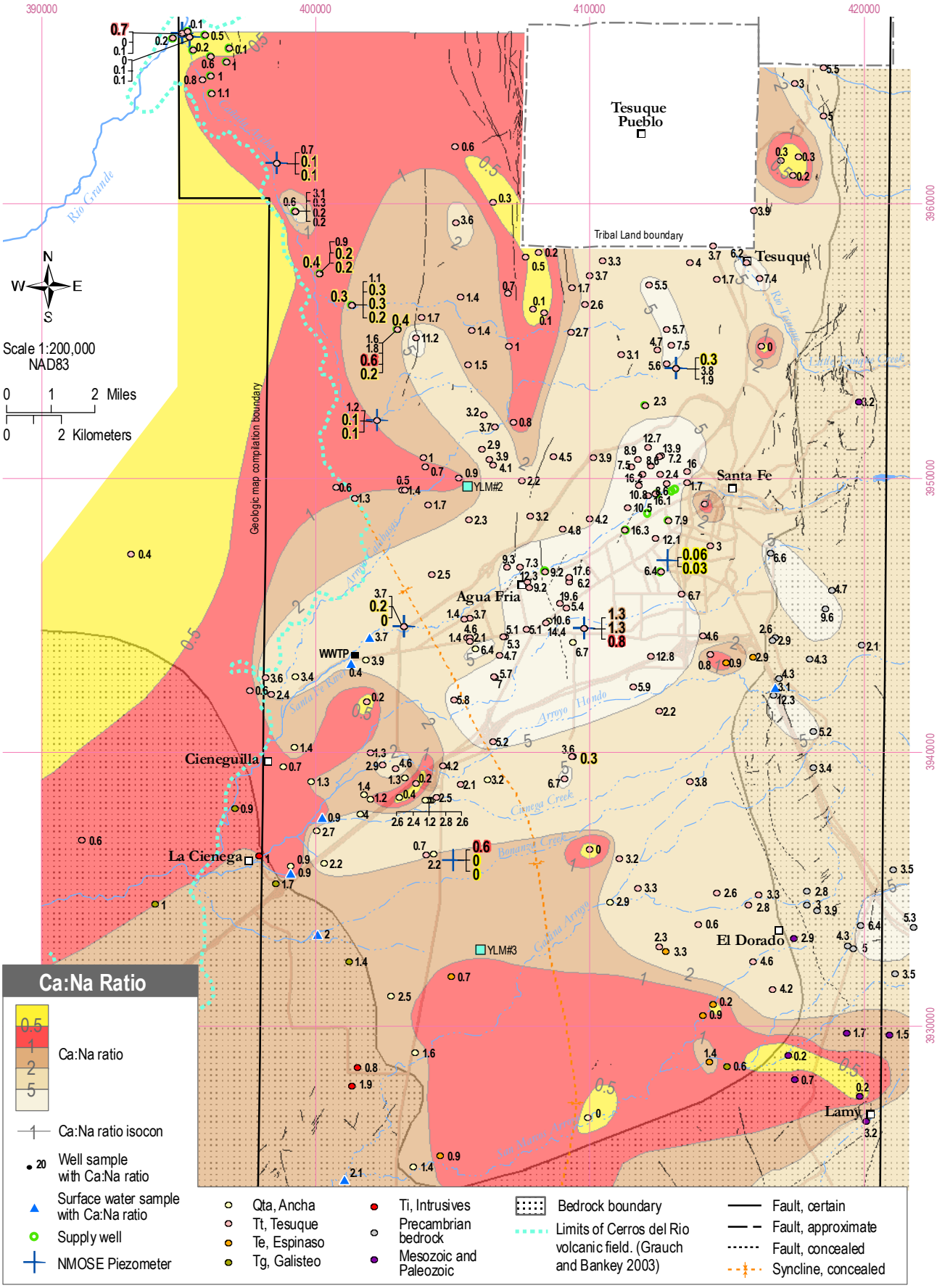

Figure 22– Ratio of calcium to sodium concentration (meq/L) for ground water in the southern Española Basin.

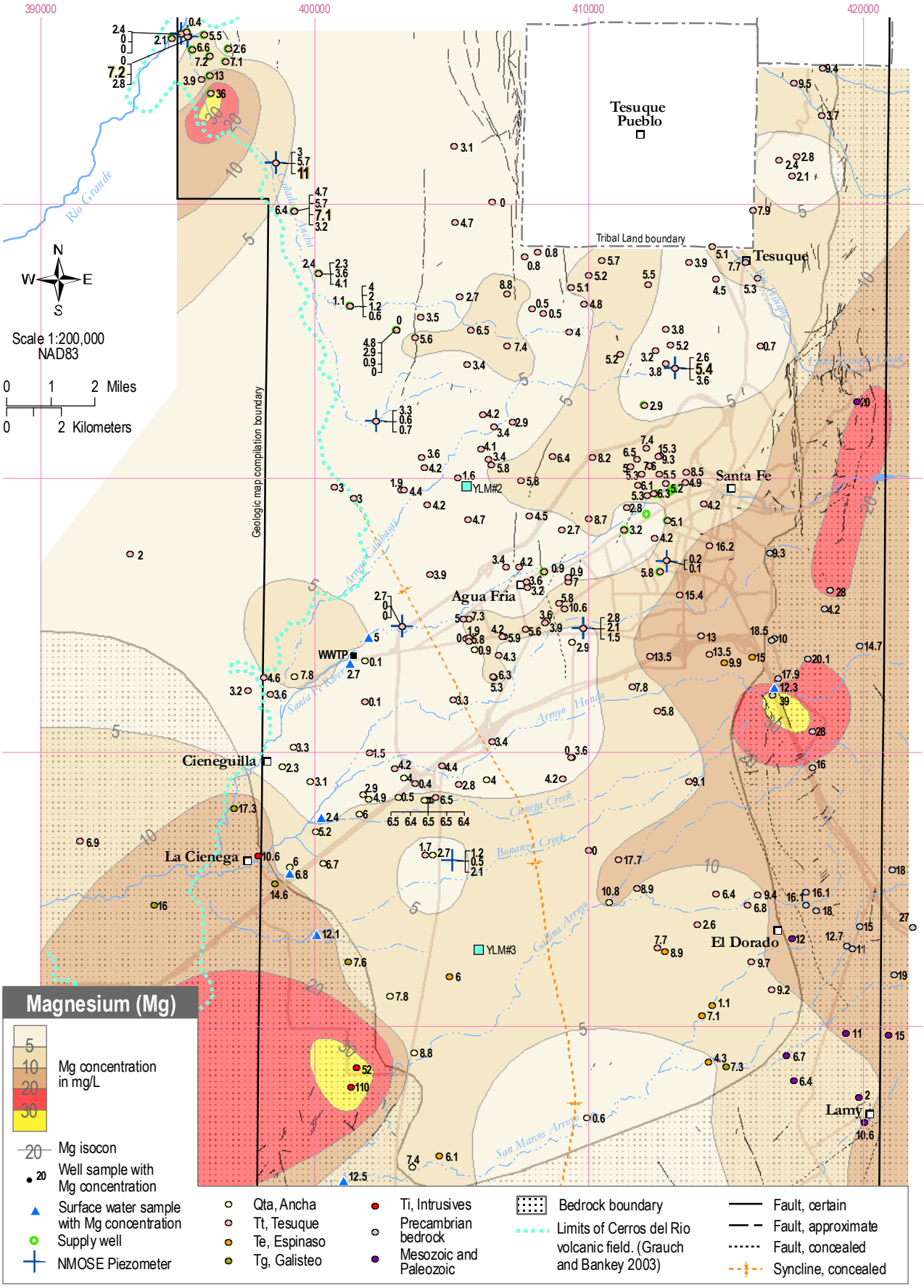

Figure 23– Magnesium concentration for ground water in the southern Española Basin.

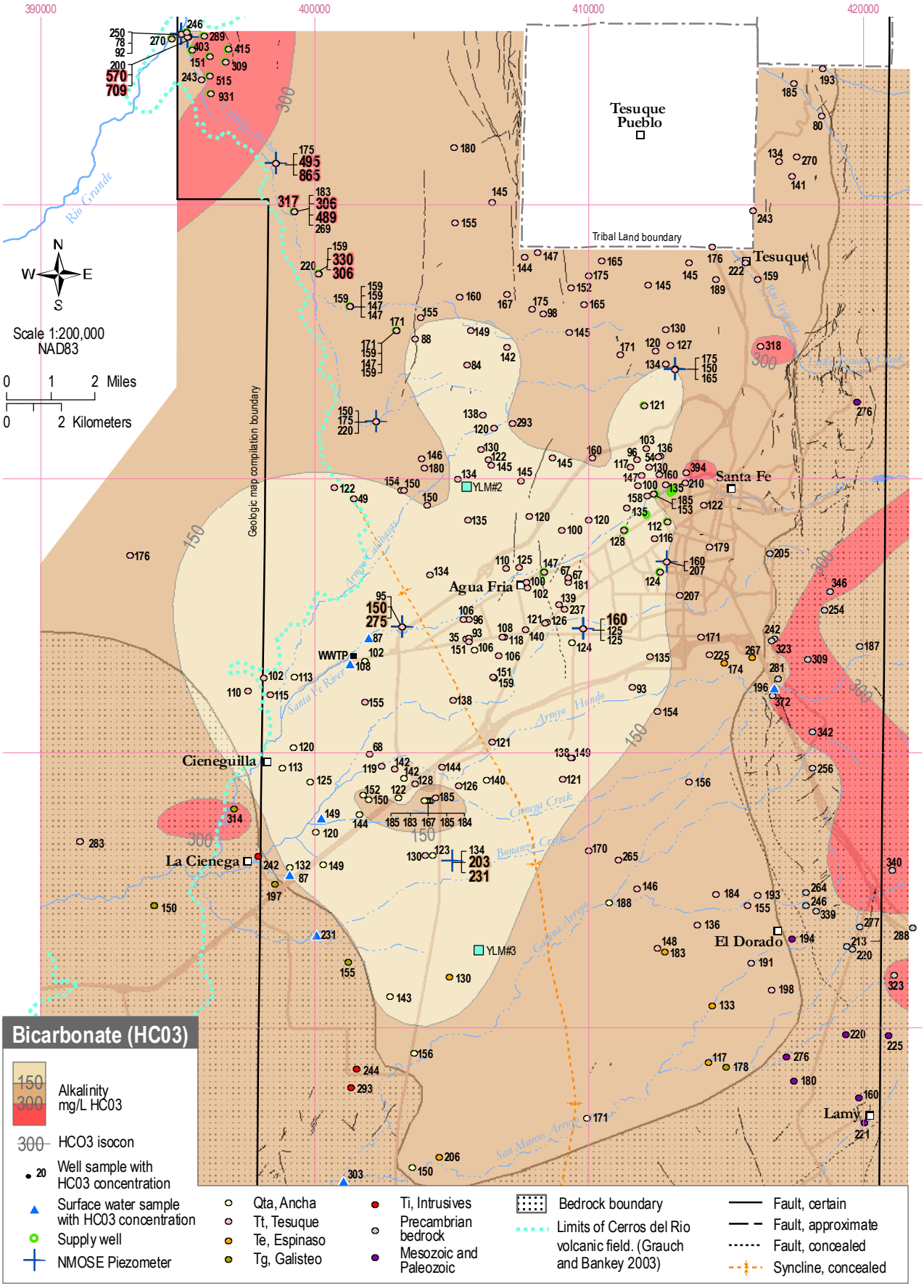

Figure 24–Bicarbonate alkalinity for ground water in the southern Española Basin.

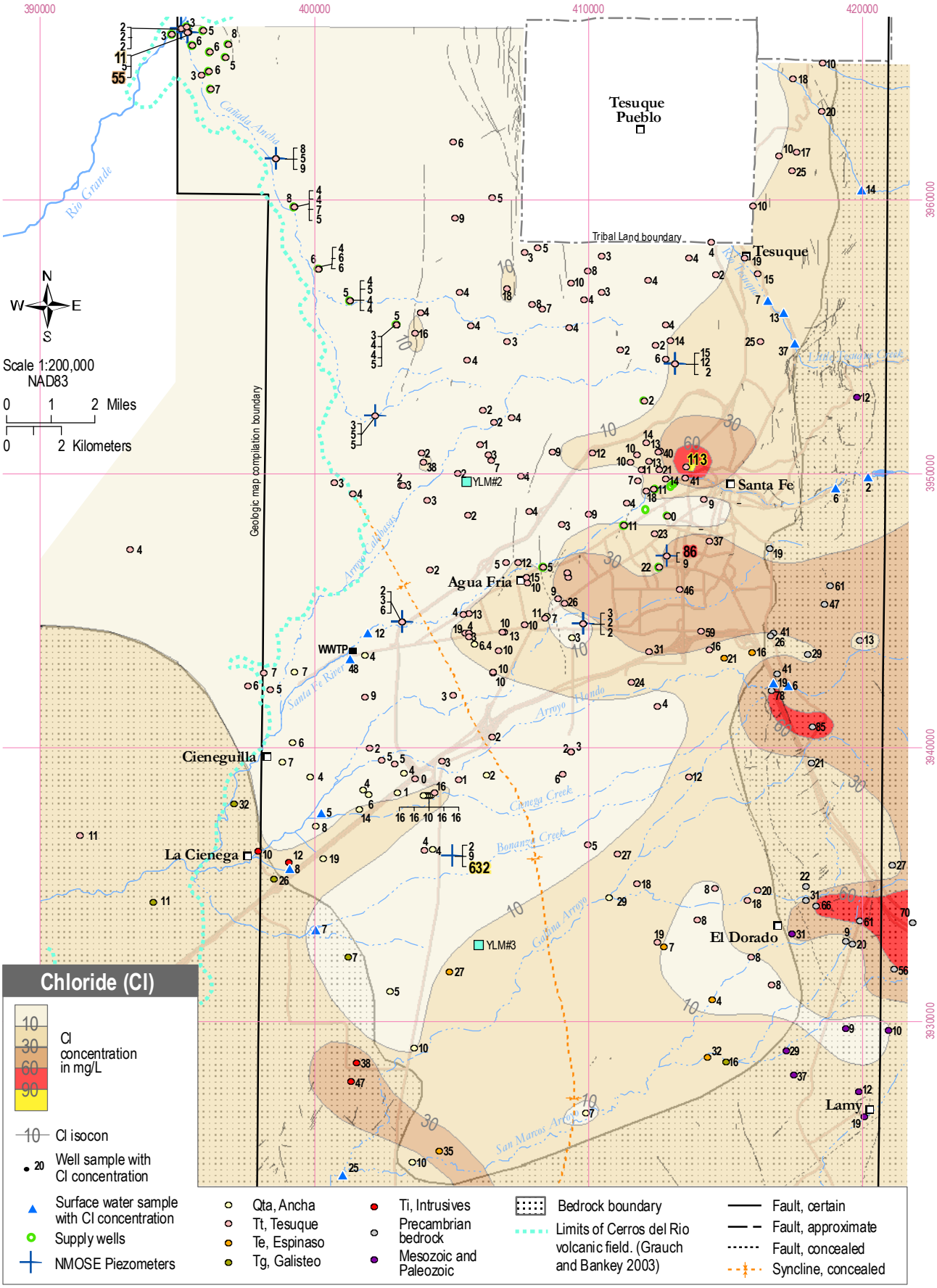

Figure 25–Chloride concentration for ground water in the southern Española Basin.

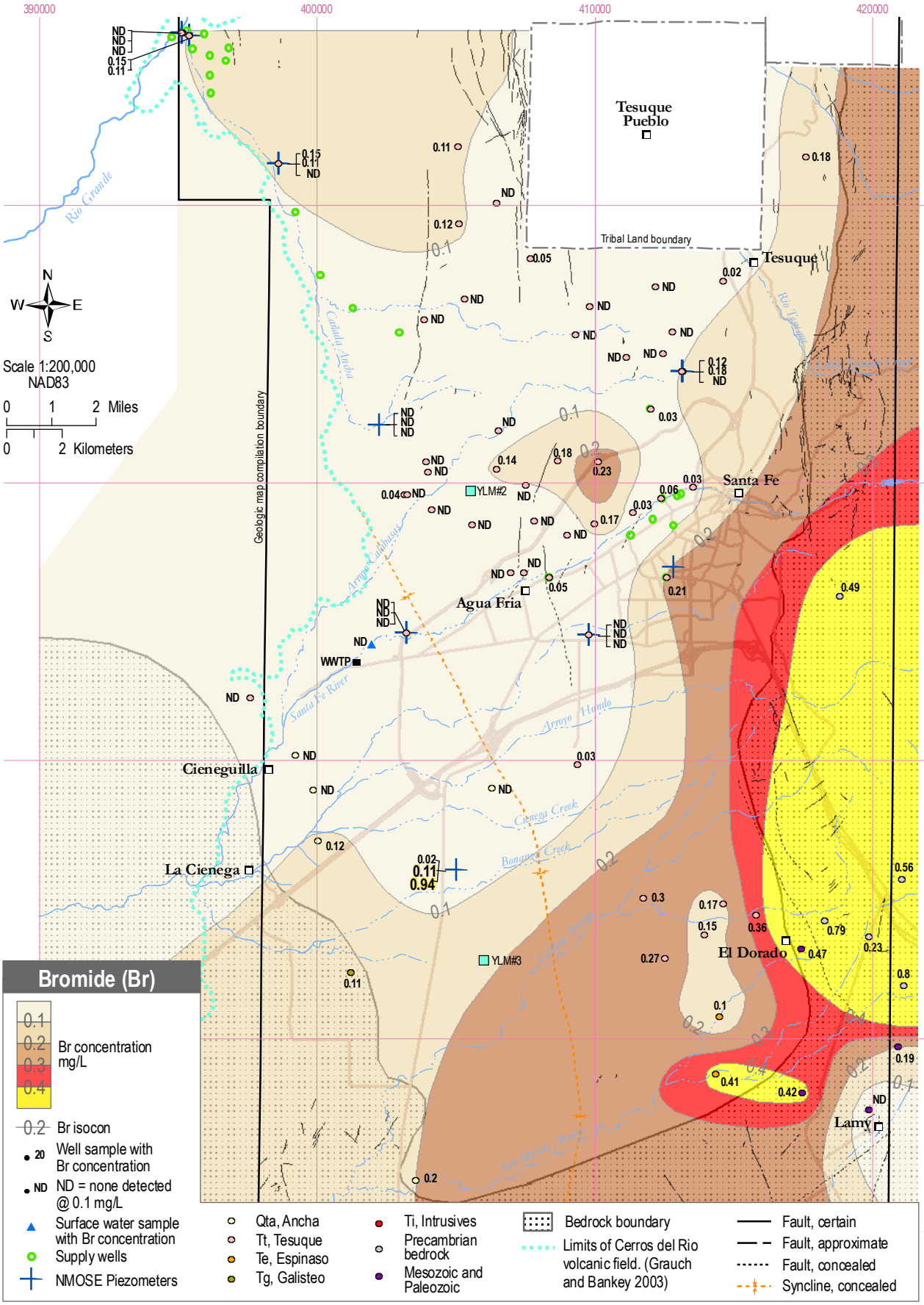

Figure 26–Bromide concentration for ground water in the southern Española Basin.

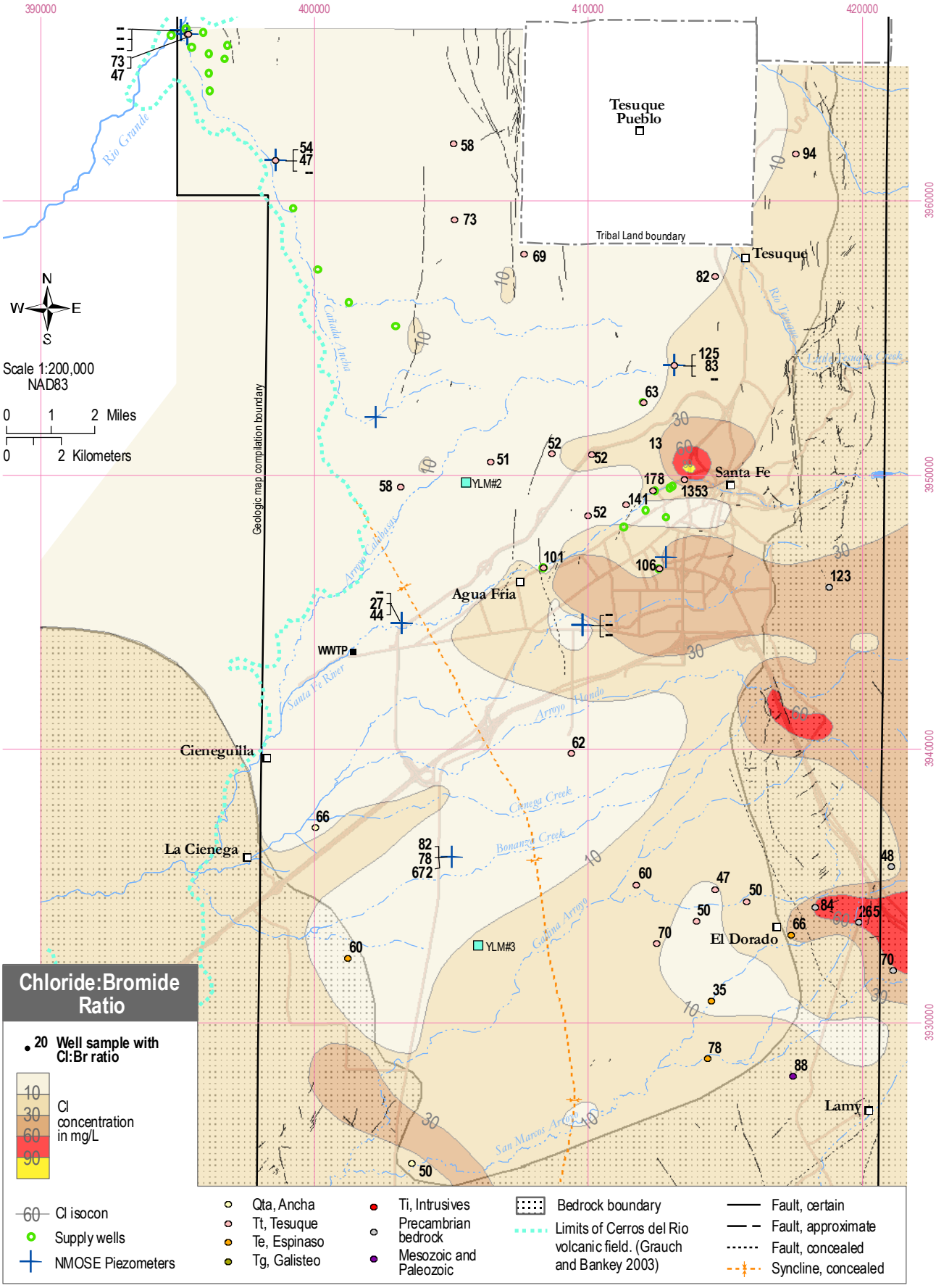

Figure 27–Ratio of chloride to bromide concentration (mg/L) and chloride concentration contours for ground water in the southern Española Basin.

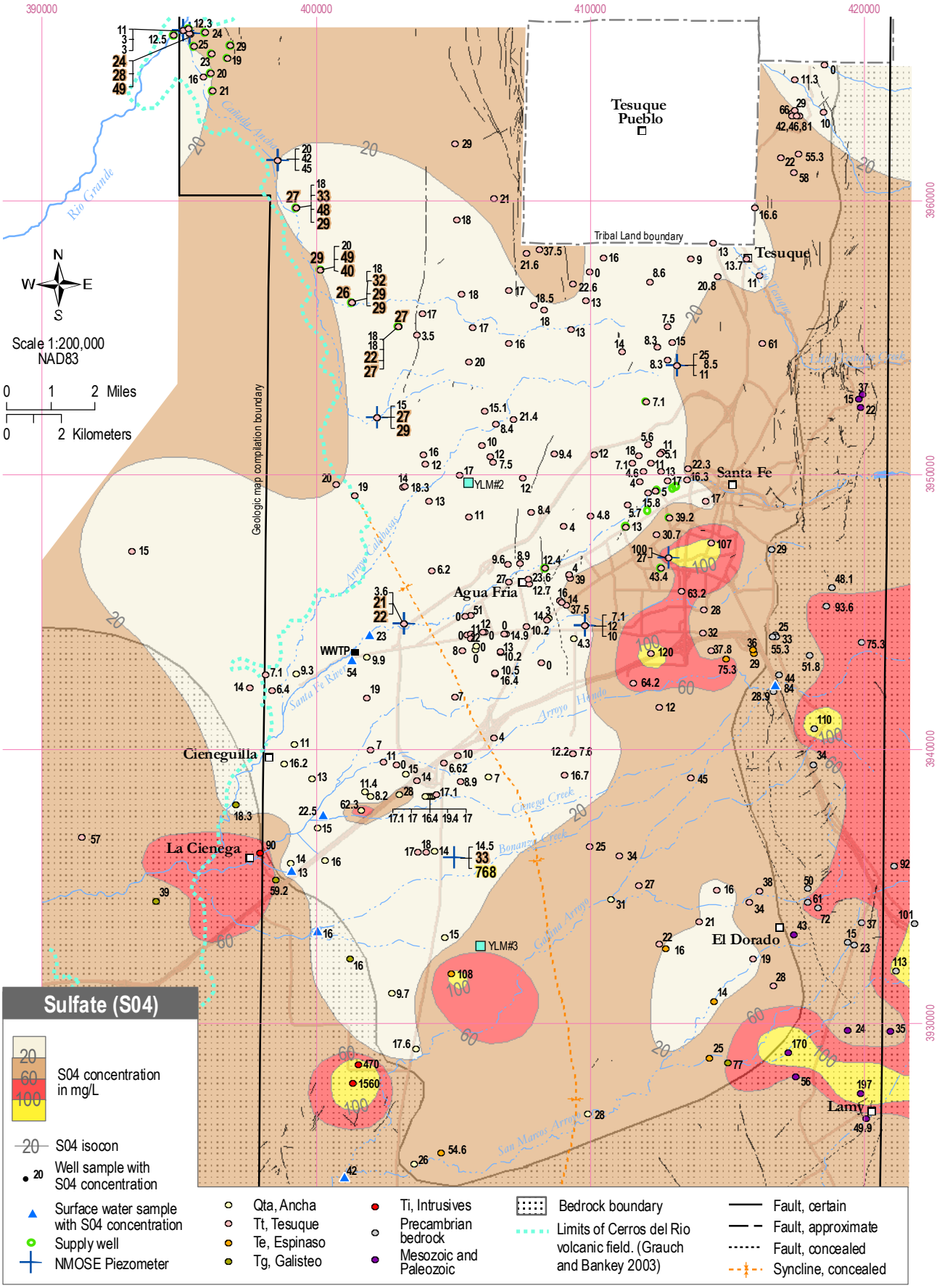

Figure 28– Sulfate concentration for ground water in the southern Española Basin.

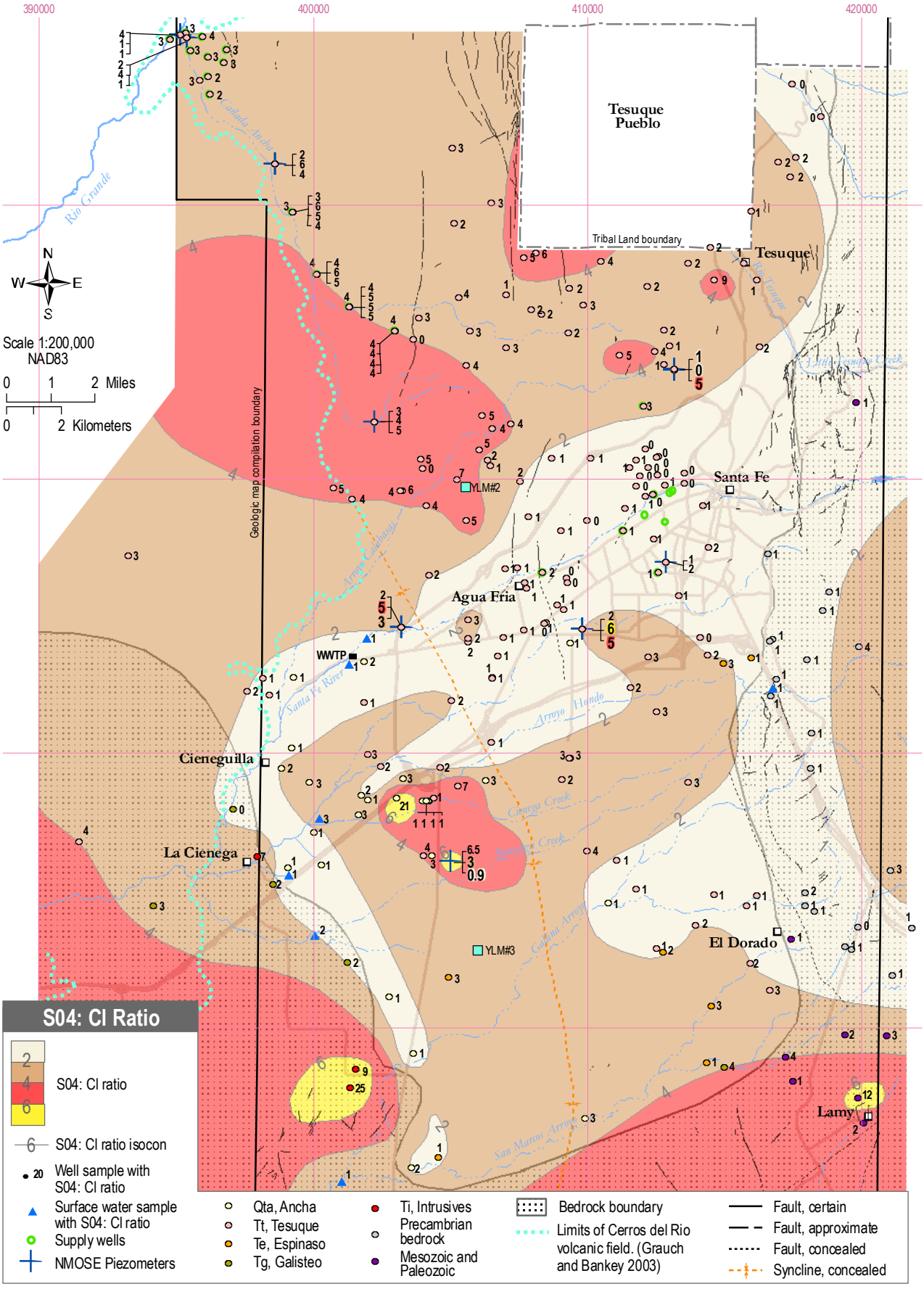

Figure 29–Ratio of sulfate (S04) to chloride (Cl) concentration (meq/L) for ground water in the southern Española Basin.

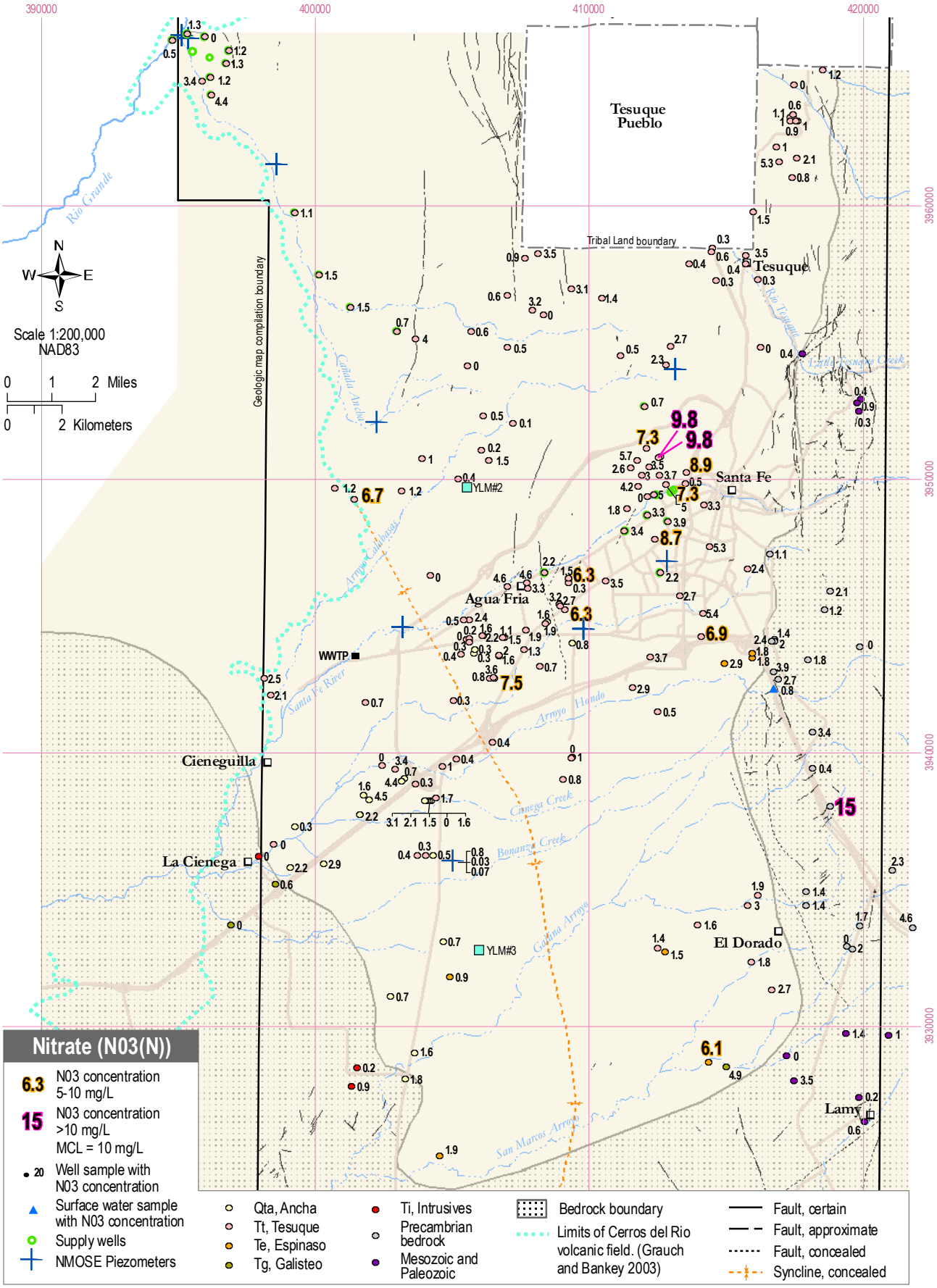

Figure 30–Nitrate (as N) concentration for ground water in the southern Española Basin.

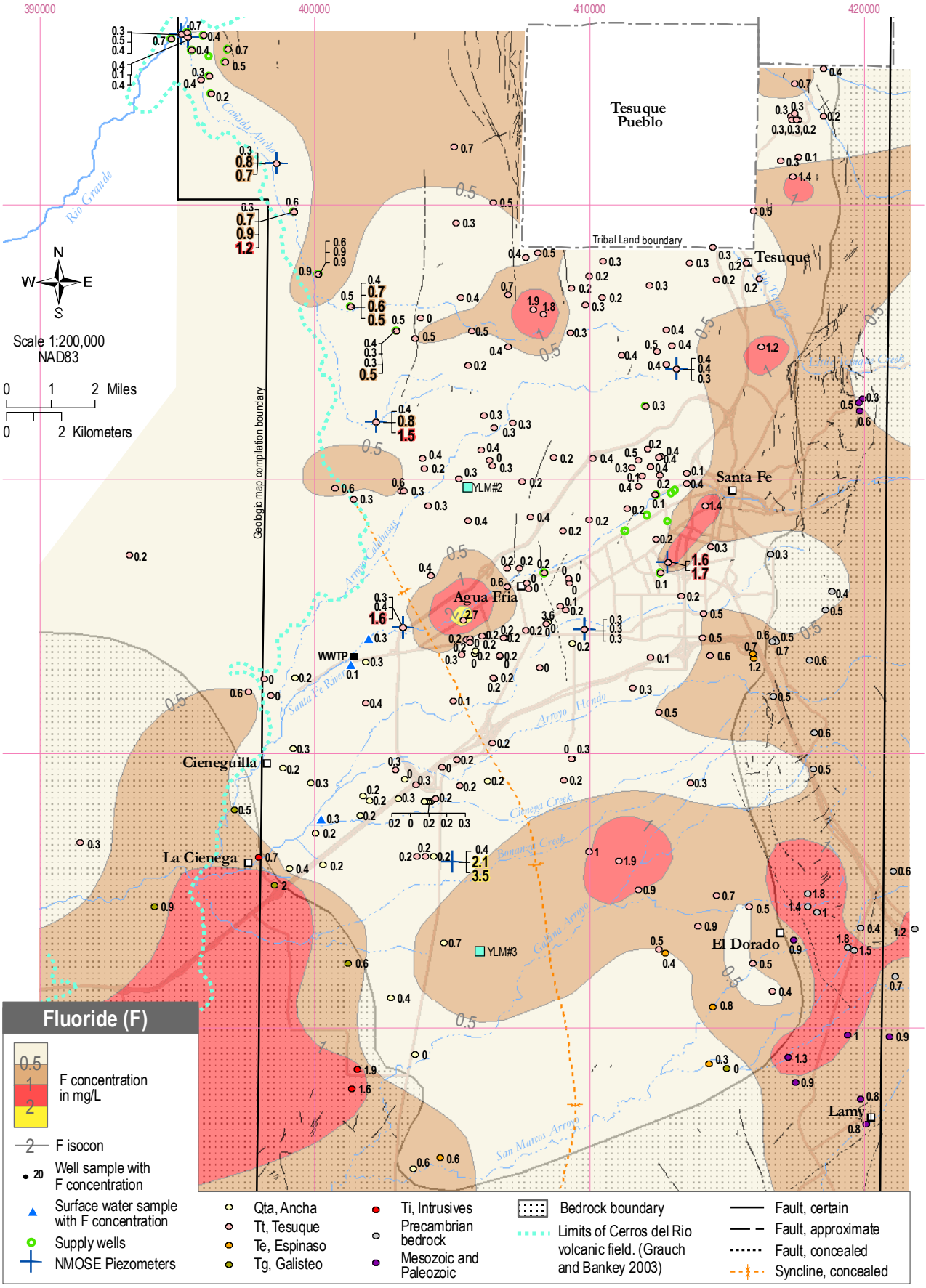

Figure 31–Fluoride concentration for ground water in the southern Española Basin.

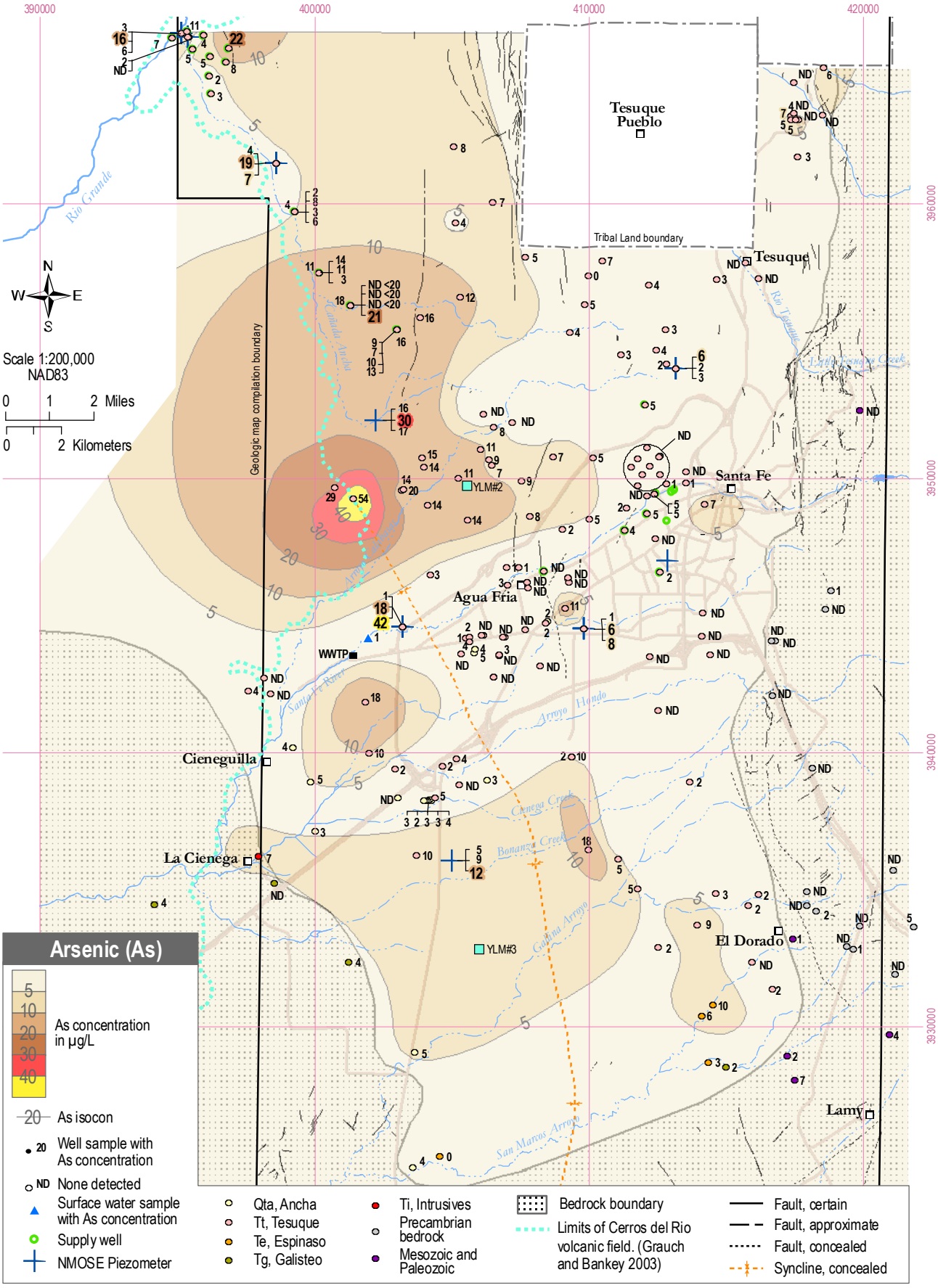

Figure 32–Arsenic concentration for ground water in the southern Española Basin.

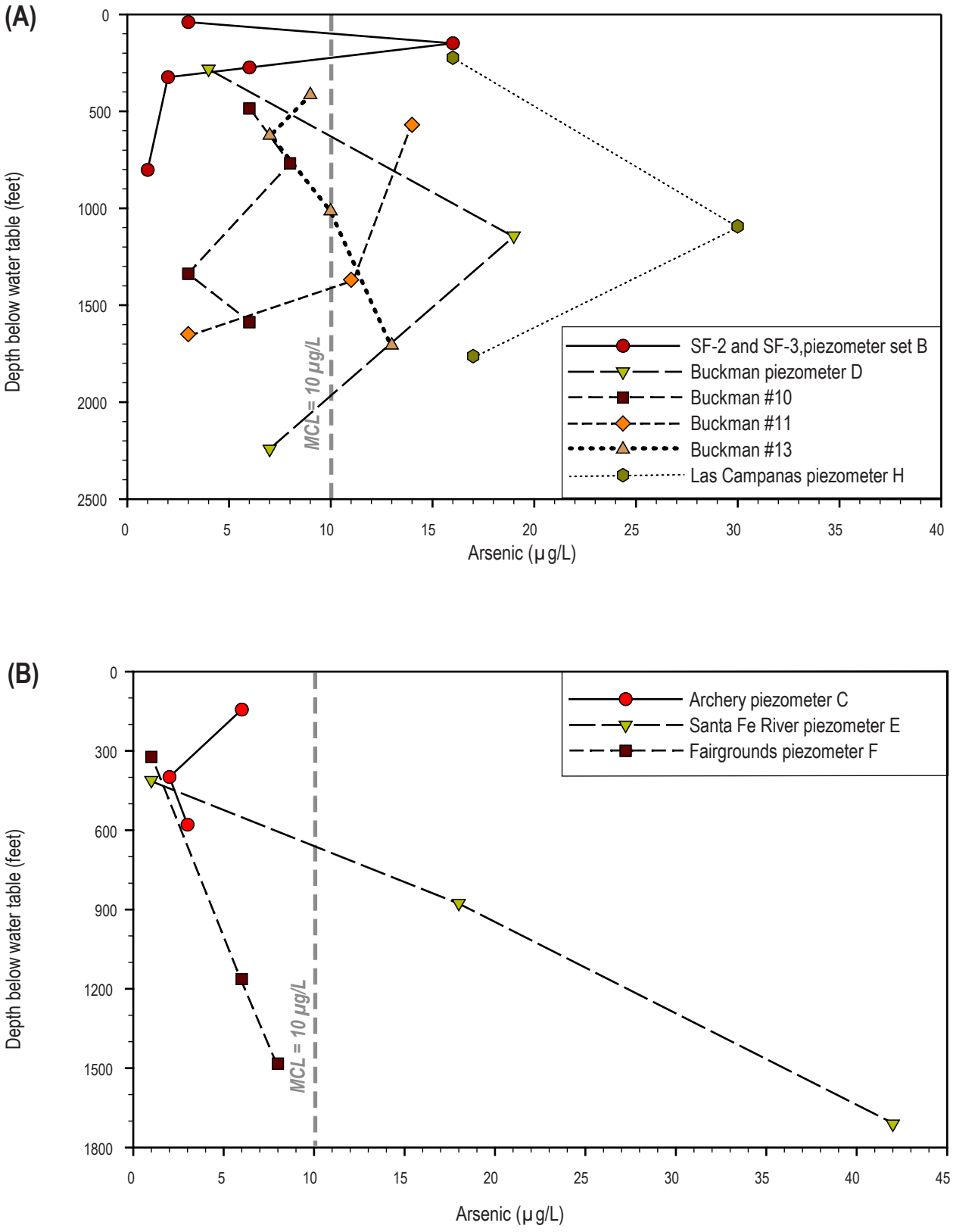

Figure 33–Variation in arsenic concentration with depth in piezometer nests located near (A) Buckman and (B) Santa Fe.

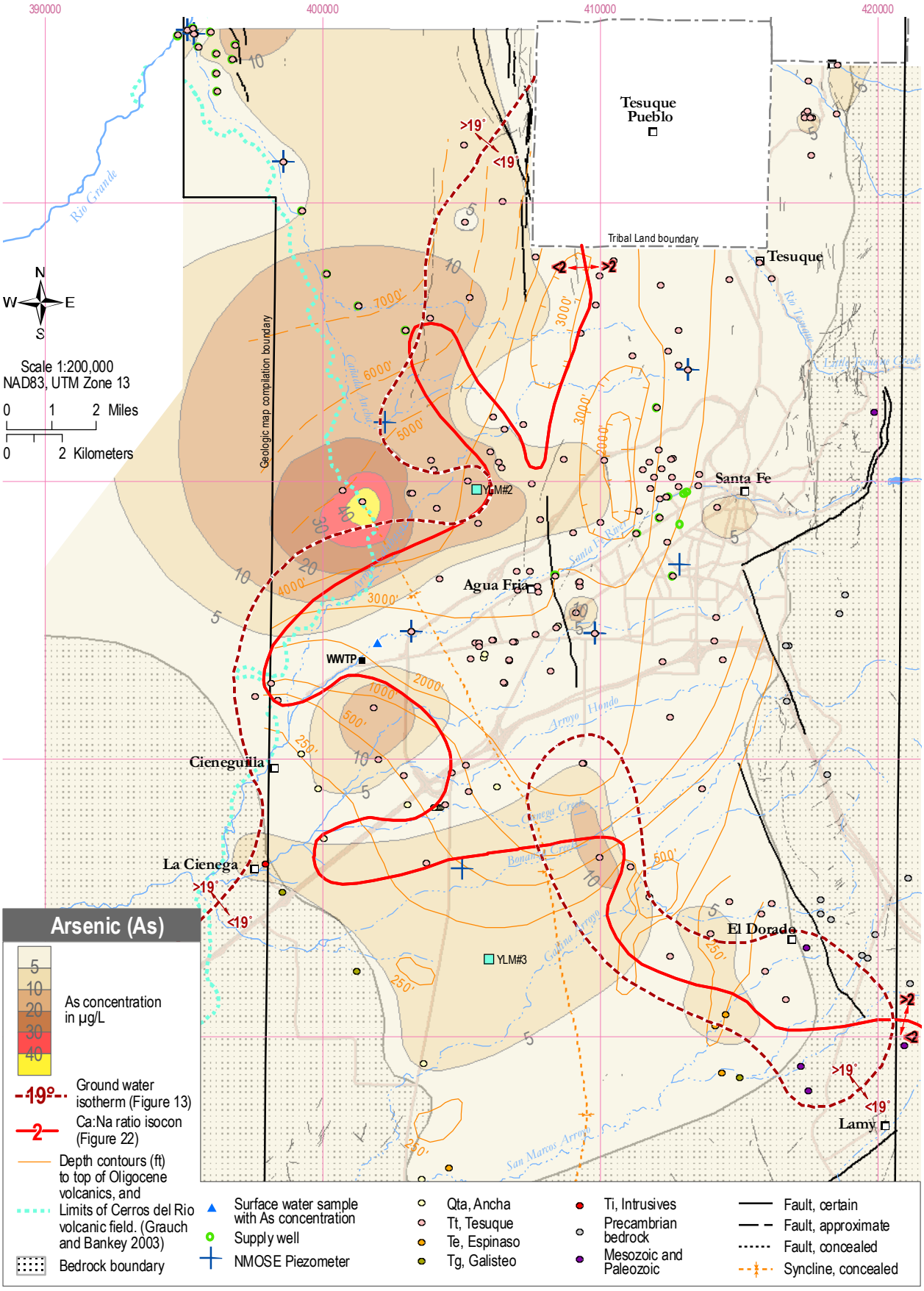

Figure 34–Spatial correlation of high arsenic concentration with elevated ground water temperature and sodium concentration.

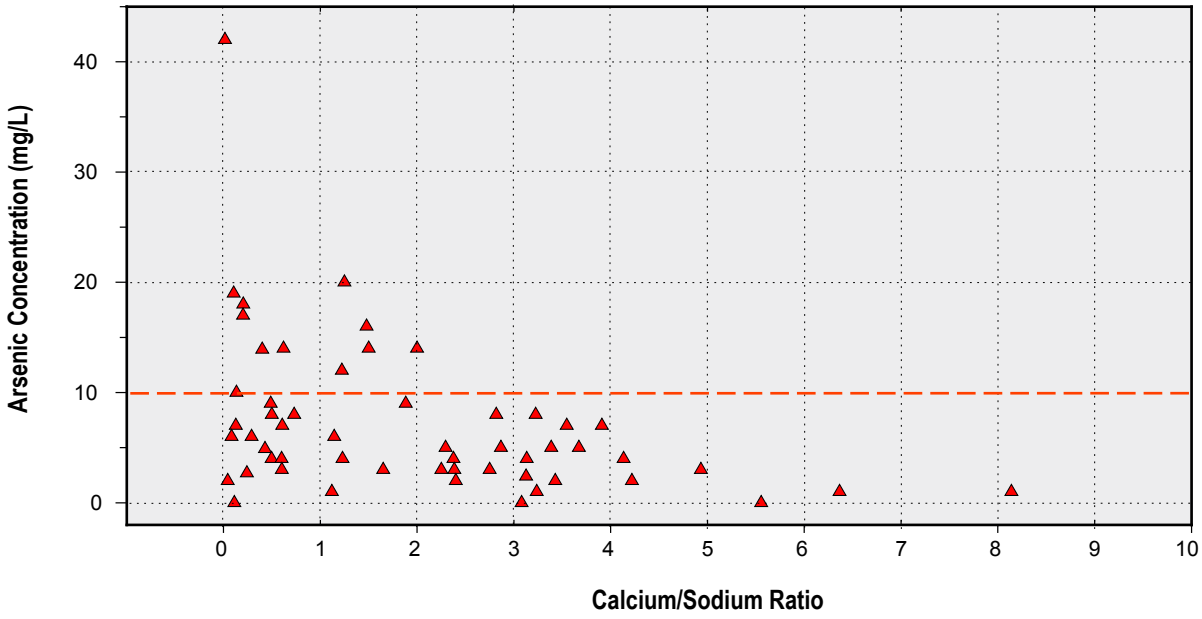

Figure 35–Plot of arsenic concentration and calcium-to-sodium ratio. All arsenic samples with concentrations above 10 µg/L occur in sodium-rich water with a Ca:Na ratio less than 2. Lower arsenic concentrations occur across a range of cation ratios.

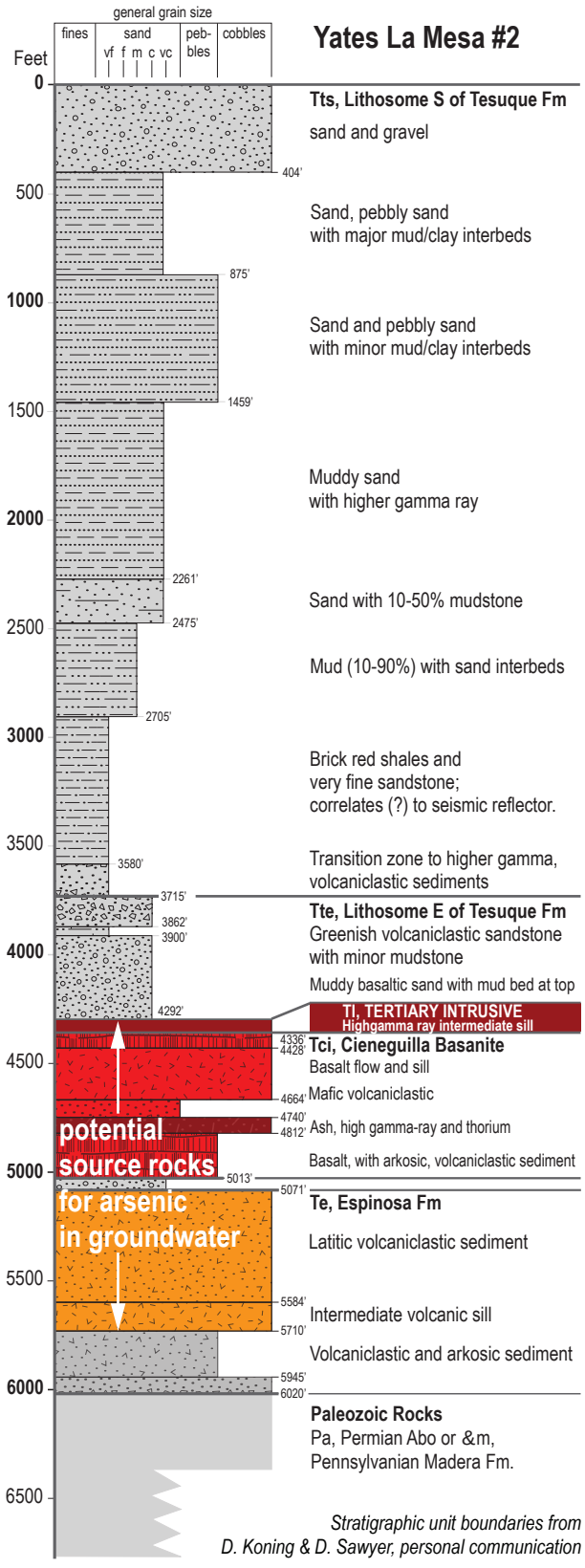

Figure 36–Generalized stratigraphic column for Yates La Mesa #2, showing potential source rocks for arsenic in ground water west of Santa Fe.

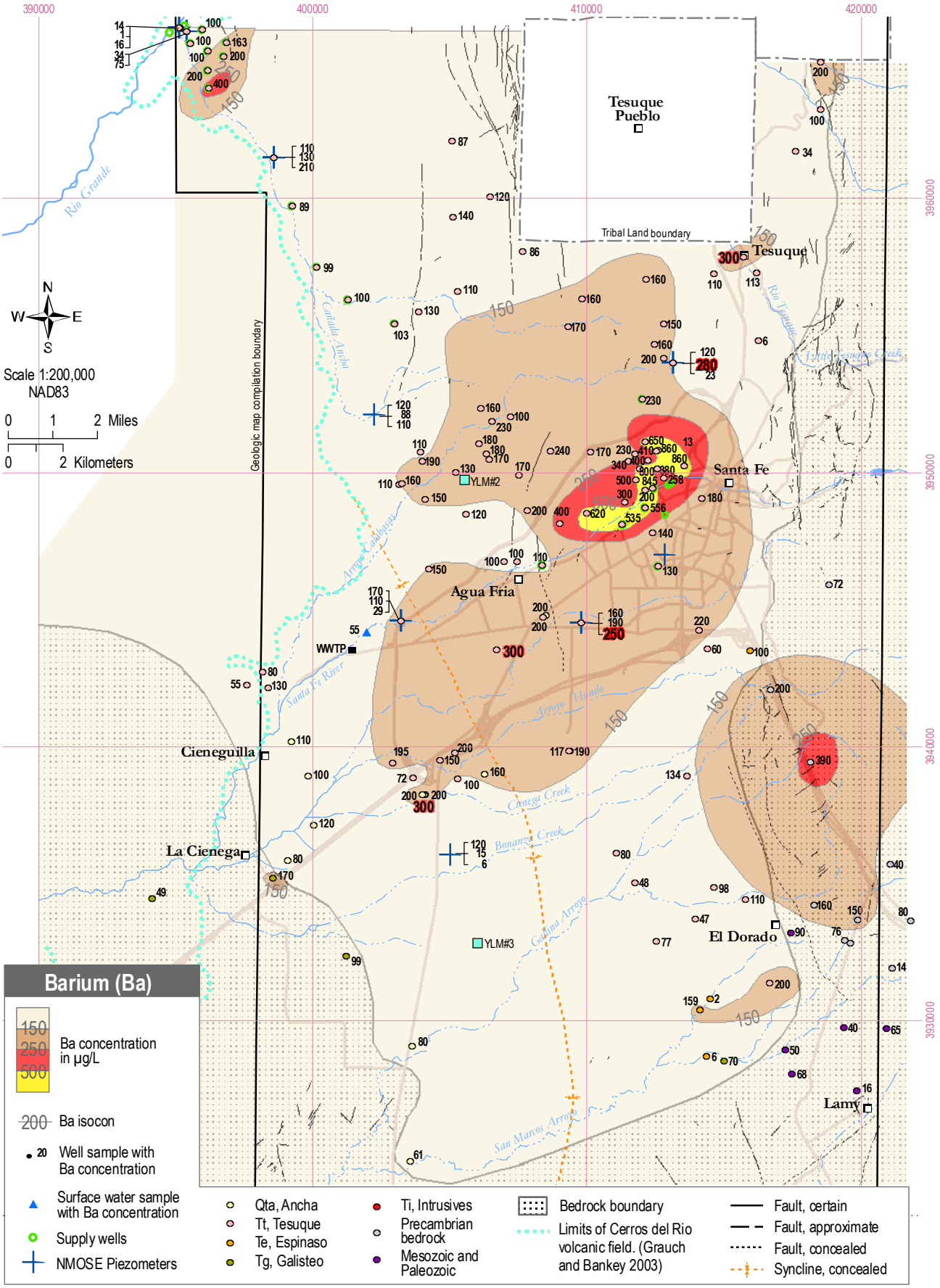

Figure 37–Barium concentration for ground water in the southern Española Basin.

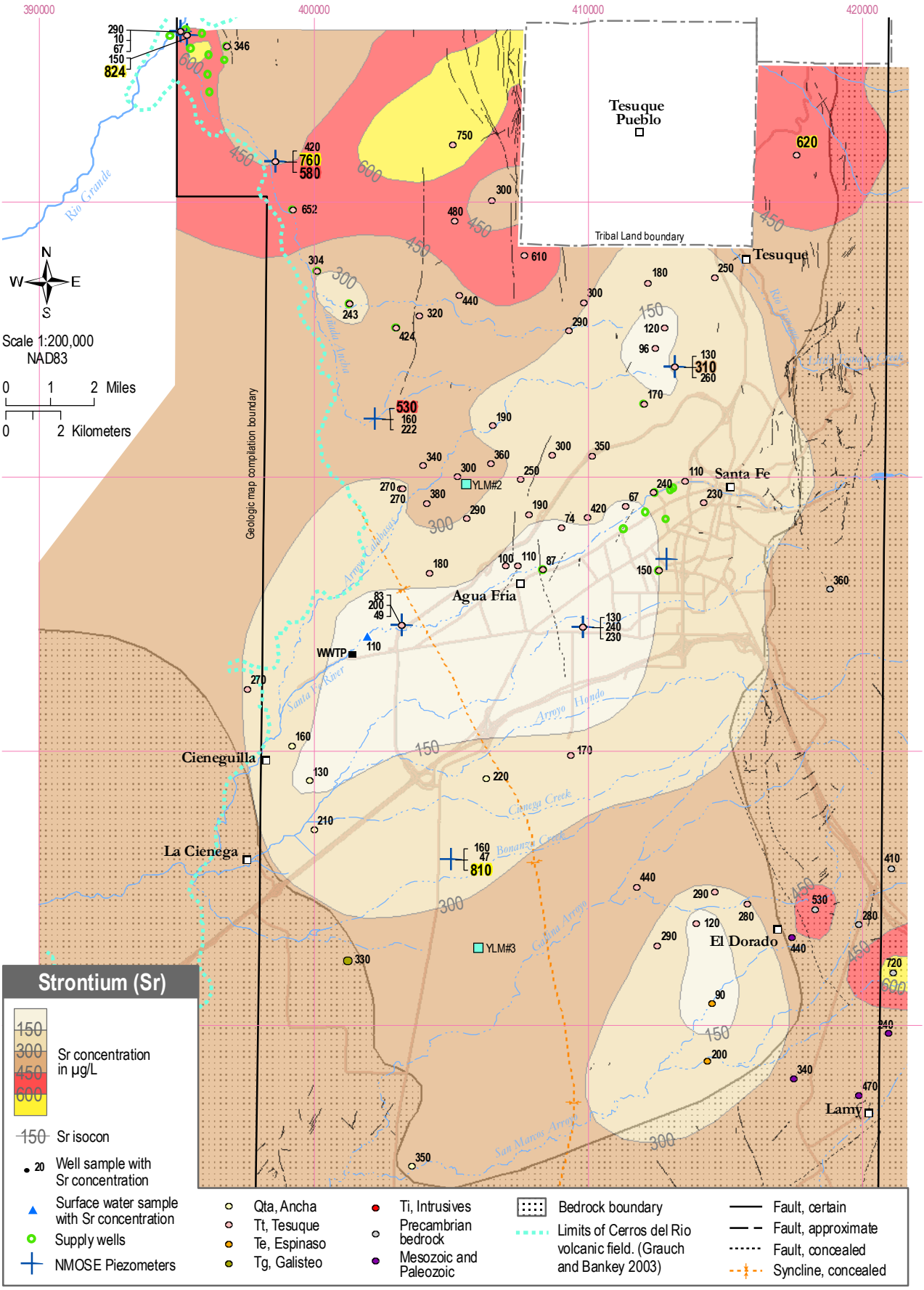

Figure 38–Strontium concentration for ground water in the southern Española Basin.

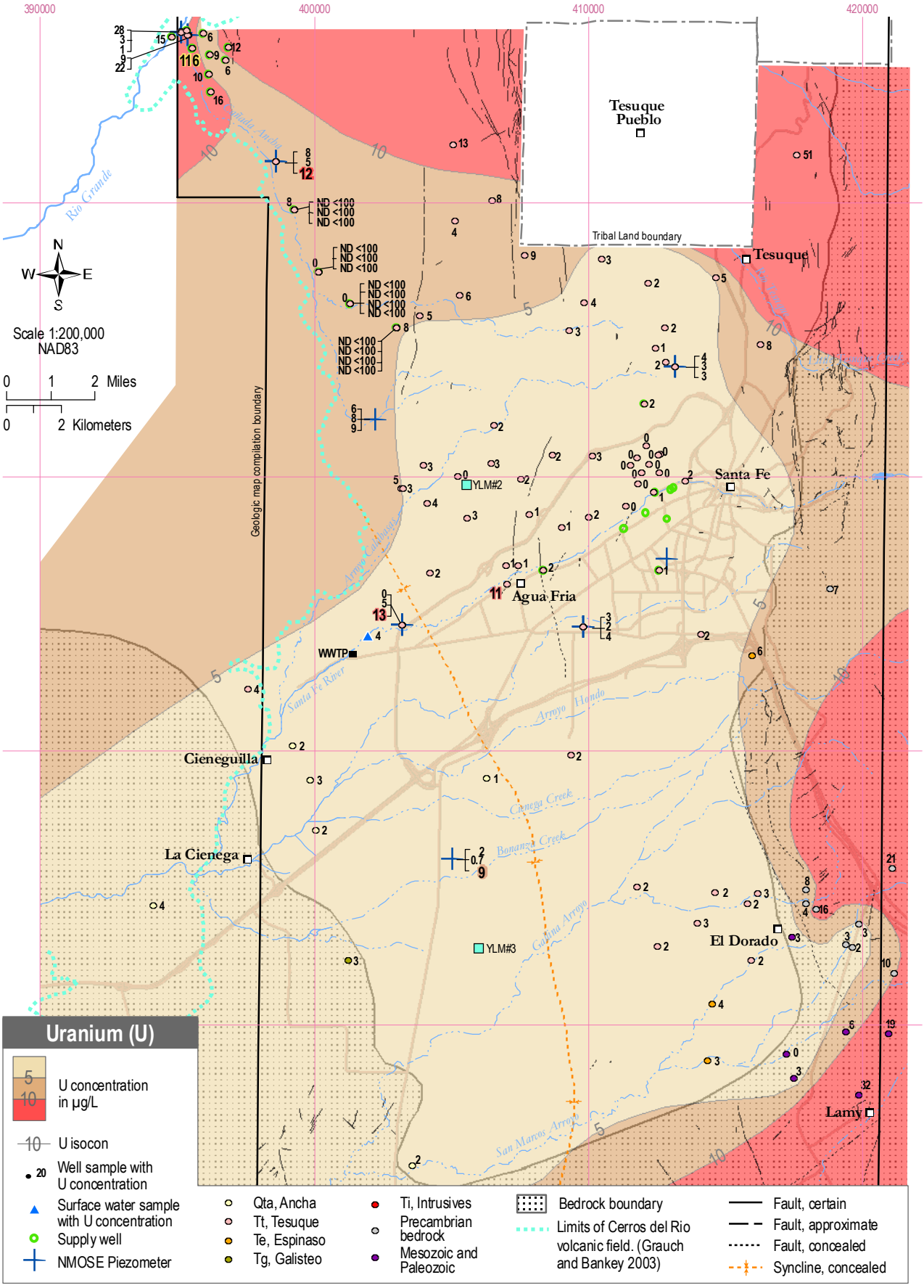

Figure 39–Uranium concentration for ground water in the southern Española Basin.

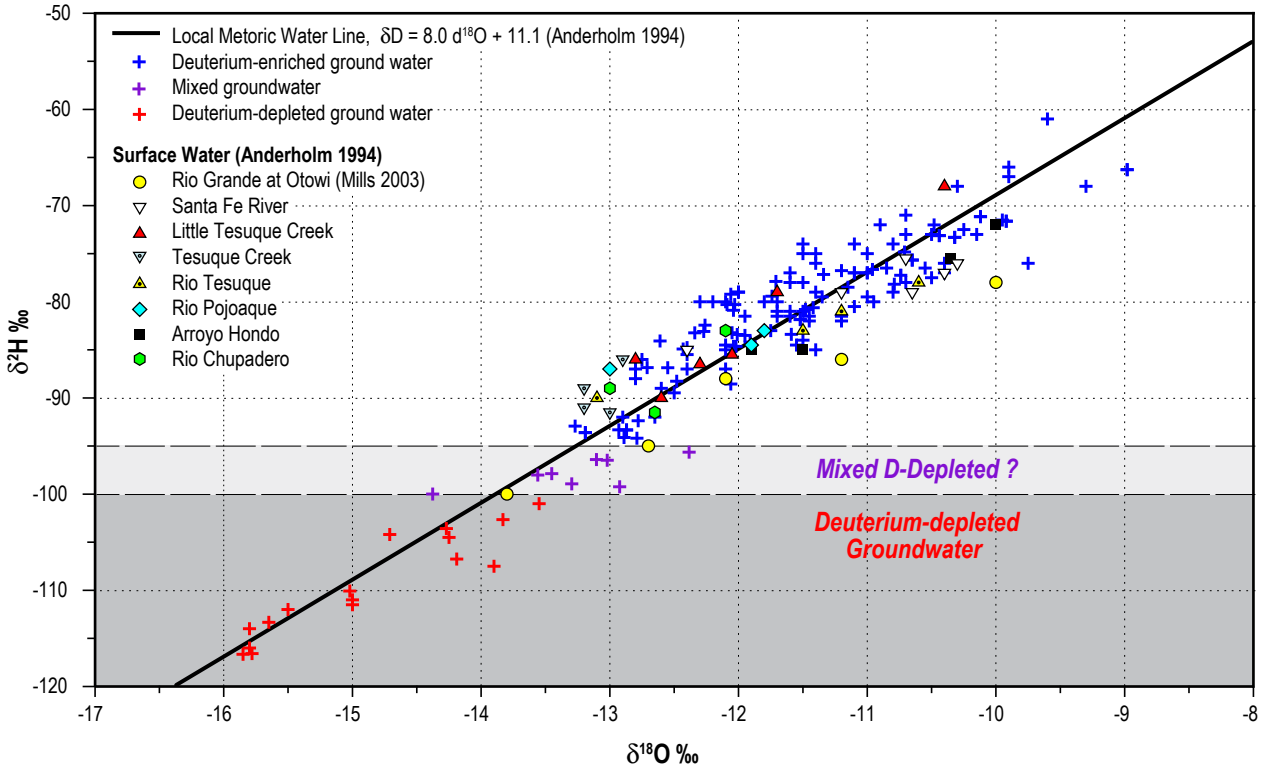

Figure 40–Values of $\delta^{2}H$ and $\delta^{18}O$ isotopic composition for all ground water and surface water samples from the southern Española Basin in relation to the local meteoric water line of Anderholm (1994)

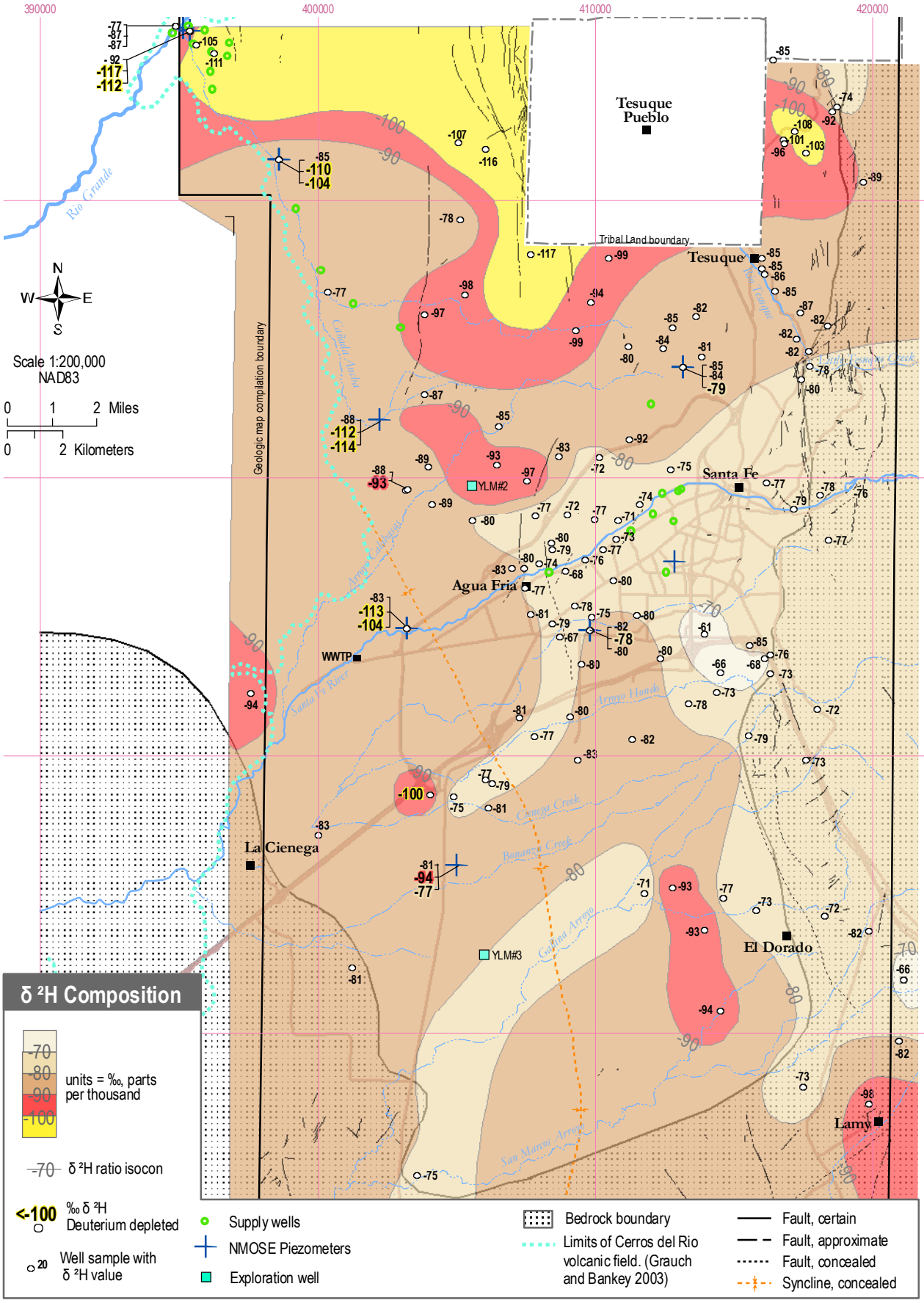

Figure 41–Stable hydrogen isotopic composition, δ ²H, for ground water in the southern Española Basin.

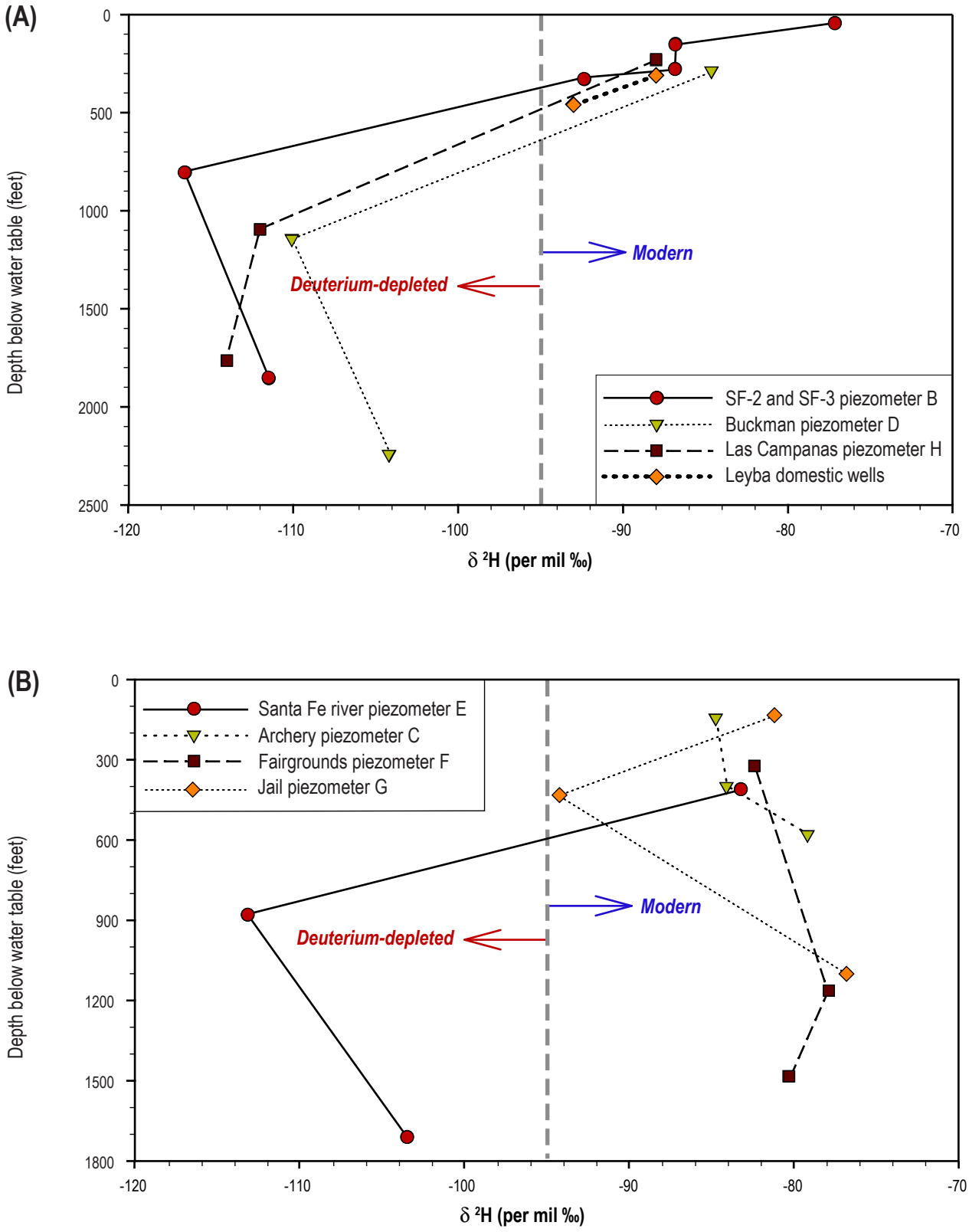

Figure 42–Variation in stable hydrogen, $\delta\,^{2}H$, composition with depth in multiple completion piezometer nests near (A) Buckman and (B) Santa Fe.

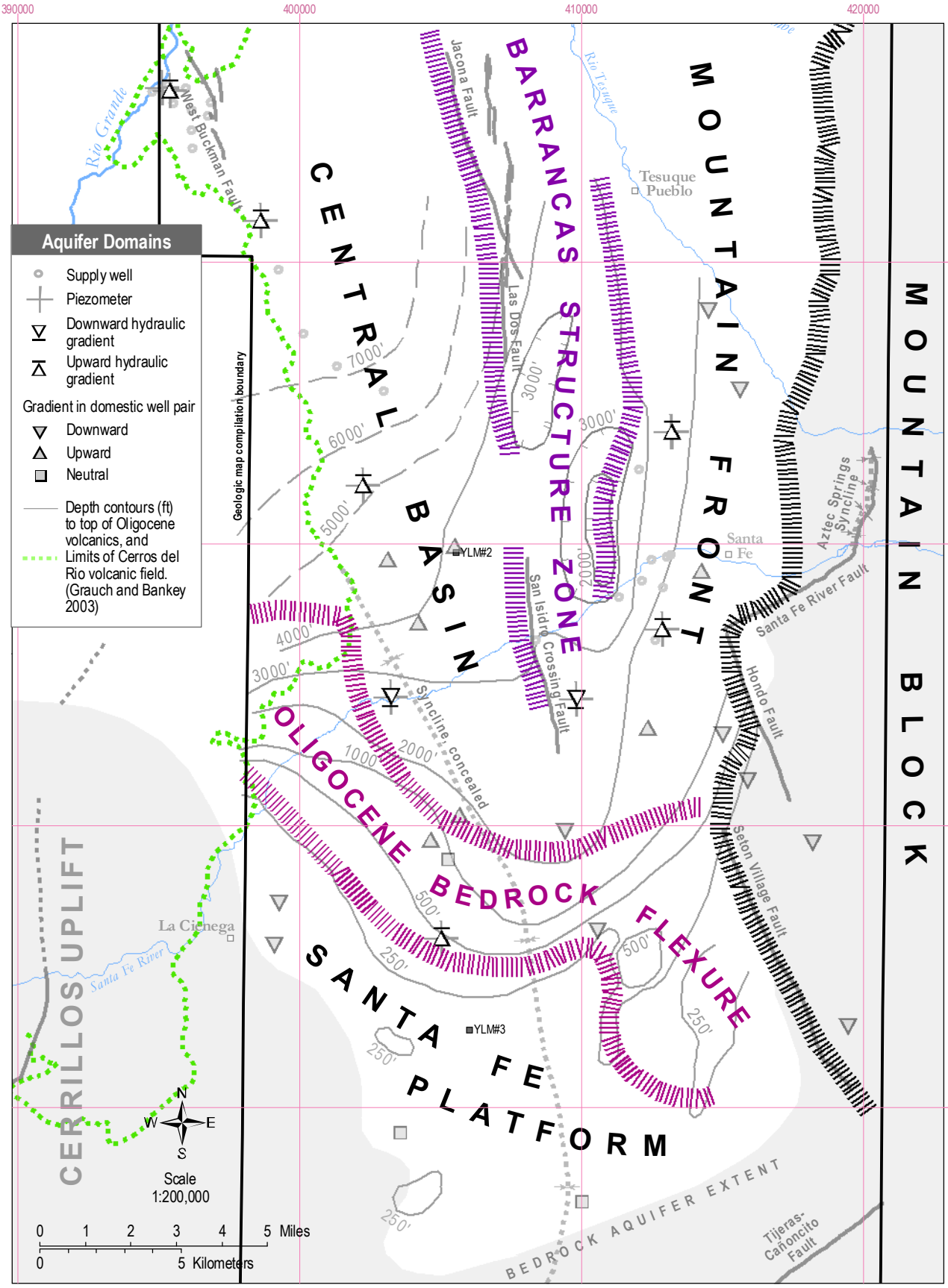

Figure 43–Aquifer compartmentalization and ground water flow domains in the Tesuque Aquifer System.